Dovepress
Taylor & Francis Group

ORIGINAL RESEARCH

Glioma-Associated Mesenchymal Stromal/Stem Cells Derived Exosomal miR-191 Promotes the Proneural-to-Mesenchymal Transition in Glioblastoma Cells via PTEN/PI3K/AKT Signaling

Peng Lv[1,2,*], Yanbin Zhang[1,3,*], Zhen Zhao[1,*], Wenjie Wu[1,*], Yan Zhou[1], Zhen Liu[1], Haofei Wang[1], Xiaobing Jiang[1], Sumeng Li[4], Pengfei Yan[1], Xing Huang[1], Wei Xiang [1], Peng Fu [1]

[1]Department of Neurosurgery, Union Hospital, Tongji Medical College, Huazhong University of Science and Technology, Wuhan, 430022, People's Republic of China; [2]Department of Rehabilitation, Tongji Hospital, Tongji Medical College, Huazhong University of Science and Technology, Wuhan, 430022, People's Republic of China; [3]Department of Plastic Surgery, Hubei Provincial Hospital of TCM, Wuhan, 430061, People's Republic of China; [4]Department of Infectious Diseases, Union Hospital, Tongji Medical College, Huazhong University of Science and Technology, Wuhan, 430022, People's Republic of China

*These authors contributed equally to this work

Correspondence: Peng Fu; Wei Xiang, Department of Neurosurgery, Union Hospital, Jiefang Avenue No. 1277, Wuhan, Hubei, 430022, People's Republic of China, Tel +86 27 85350819, Email pfu@hust.edu.cn; xiangwei20@hotmail.com

Background: The proneural-to-mesenchymal transition (PMT) represents a crucial phenotypic transformation in glioblastoma. Glioma-associated mesenchymal stromal/stem cells (GaMSCs) play a significant role in diverse biological processes of gliomas. However, the impact of exosomes released from GaMSCs (GaMSCs-Exos) on the PMT of glioblastoma remains inadequately understood. This study aimed to explore the effects and mechanisms of GaMSCs-derived exosomal miRNA-191-5p on the PMT of glioblastoma.

Methods and Results: Conditioned medium from three independently established GaMSCs lines (GaMSCs-CM) significantly enhanced the tumorigenicity of glioma cells. Further analysis demonstrated that GaMSC-Exos, isolated from GaMSCs-CM, promoted both the tumorigenicity and PMT of glioma cells, both in vitro and in vivo. Exosomal miR-191-5p derived from GaMSCs was identified as the principal mediator. Overexpression and inhibition of miR-191-5p affected the tumorigenicity and PMT of glioma cells, in both laboratory and animal models. Bioinformatics analyses and luciferase reporter assays confirmed that miR-191-5p targets PTEN. Additionally, rescue experiments indicated that increased PTEN expression could reverse the effects of miR-191-5p overexpression on tumorigenicity and PMT through modulation of the PI3K/AKT signaling pathway.

Conclusion: Our findings highlight the role of GaMSC-Exos in mediating the intercellular transfer of miRNA-191-5p, which facilitates the PMT of glioma. The process underlying the enhanced aggressiveness and PMT is driven by miR-191-5p, promoting glioma progression by targeting PTEN and activating the PI3K/AKT signaling pathway.

Keywords: glioma-associated mesenchymal stromal/stem cells, exosomes, proneural to mesenchymal transition, miR-191-5p

Introduction

Glioblastoma multiforme (GBM) represents the most prevalent primary malignant tumor of the central nervous system in adults.[1] Despite significant advancements in surgical techniques and neoadjuvant chemoradiotherapy over recent decades, the clinical outcomes and prognosis for patients with glioblastoma remain dismal, with an overall 5-year survival rate of less than 5%.[2] Through integrated genomic and transcriptomic analyses, GBM can be classified into three intrinsic molecular subtypes: mesenchymal (MES), classical (CL), and proneural (PN).[3] The PN subtype is associated with a relatively favorable prognosis compared to other subtypes, whereas the MES subtype is characterized by increased aggressiveness and immune evasion. Consequently, the MES subtype is notably characterized by poor prognosis and

resistance to therapeutic interventions.[4] One critical process in the development of GBM is the proneural-to-mesench-ymal transition (PMT), which correlates with a poorer prognosis and heightened resistance to standard treatments.[5] A deeper understanding of the complex network of molecular events that govern PMT is essential for the development of targeted therapies designed to hinder or reverse this transition.

Mesenchymal stem cells (MSCs), a type of stromal cell characterized by low immunogenicity and possessing chemotactic and immune-regulatory properties, play a pivotal role in the tumor microenvironment (TME).[6] Triggered by cytokines released by tumor cells and their surrounding matrix, MSCs are recruited to the TME, where they participate in various facets of tumor progression.[7] Glioma-associated mesenchymal stromal/stem cells (GaMSCs), important mesenchymal cells within the glioma microenvironment, originate from MSCs recruited from normal tissue to the tumor niche. GaMSCs express MSC surface markers such as CD105, CD73, CD90, and CD44, while lacking expression of CD31, CD34, and CD14. Moreover, GaMSCs have the capacity to differentiate into various cell types under specific conditions, including adipocytes, osteoblasts, and chondrocytes. Our research, along with findings from other groups, demonstrates that GaMSCs not only promote tumor cell proliferation, invasion, and drug resistance, but also play a significant role in glioma angiogenesis.[8–13] GaMSCs secrete angiogenic factors such as TGF-β1 and PDGF-BB, which stimulate tube formation and vascular development through interaction with their respective receptors on endothelial cells.[10] Furthermore, CD90(low) GaMSCs can differentiate into pericyte-like cells, contributing to vessel stabilization and structural support during the formation of new blood vessels.[14]

Exosomes, defined as small vesicles with diameters ranging from 30 to 200 nanometers, are produced and secreted by cells into the extracellular environment.[15] The functional capacity of the exosomal cargo, which comprises proteins, nucleic acids, and bioactive molecules—particularly microRNAs (miRNAs)—is contingent upon its specific constituents.[16] Recent studies have elucidated the pivotal role of exosomes in facilitating intercellular communication among tumor cells, thereby significantly influencing tumor progression, dissemination, and metastasis.[17] Additionally, prior research has demonstrated that exosomes and other factors released by GaMSCs contribute to the tumorigenicity of gliomas.[18] However, the specific role of exosomes derived from GaMSCs (GaMSC-Exos) in the PMT of glioma cells remains inadequately explored.

In our investigation, GaMSC-Exos were found to promote the PMT of glioblastoma, and GaMSC-Exos could elevated the concentration of miR-191-5p in glioma cells. Concurrently, overexpression of miR-191-5p in these cells not only augments proliferation, migration, and invasion but also significantly increases the expression of (Vimentin and CD44), while decreasing the expression of the proneural markers (Sox2 and Olig2). This alteration facilitates the PMT. Moreover, PTEN has been identified as a target of miR-191-5p derived from GaMSC-Exos, which subsequently modulates the downstream PI3K-AKT signaling pathway. These findings offer a novel perspective on the role of GaMSC-derived exosomes in promoting the PMT of glioblastoma cells and provide crucial insights into the underlying mechanisms driving the progression of gliomas.

Materials and Methods
Characteristics of Patients with Various Grades of Gliomas
This research received ethical approval from the Ethical Committee of Huazhong University of Science and Technology [2019]IEC(S561) and adhered to the Helsinki Declaration of the World Medical Association. Informed consent was obtained, and surgical tumor tissues were collected from 43 patients, aged between 20 and 63 years, with histologically confirmed glioma. The collection occurred between September 2022 and September 2023 at the Department of Neurosurgery, Union Hospital, Tongji Medical College, Huazhong University of Science and Technology. Detailed patient information is provided in Supplementary Table S1. All participants presented with primary gliomas and had not received prior radiotherapy or chemotherapy.

Establishment and Cultivation of Glioma Stem Cells (GSCs)
Human GSCs were isolated from freshly resected surgical tumor specimens from patients diagnosed with GBM, with informed consent and following ethical clearance by the Ethical Committee of Huazhong University of Science and Technology [2019]IEC(S561). The study complied with the Helsinki Declaration of the World Medical Association.

Tumor samples were rinsed in sterile phosphate-buffered saline (PBS), mechanically minced into 1–2 mm³ pieces, and enzymatically dissociated into single cells using the Papain Dissociation System (Worthington Biochemical, Lakewood, NJ, USA) according to the manufacturer's instructions. To enrich for GSCs, magnetic-activated cell sorting (MACS) was utilized. Dissociated single cells were incubated with CD133-conjugated magnetic microbeads (CD133 MicroBead Kit, Miltenyi Biotec, Bergisch Gladbach, Germany), following which CD133$^+$ cells were isolated per the manufacturer's guidelines. In some experiments, co-selection with CD15-conjugated microbeads was also performed to achieve a dual-positive CD133$^+$/CD15$^+$ population. Cells identified as CD133$^+$ or CD133$^+$/CD15$^+$ were considered putative GSCs, whereas CD133$^-$/CD15$^-$ cells served as non-stem tumor cells.[19,20] Isolated GSCs were cultured in serum-free DMEM/F12 medium (Gibco, Waltham, MA, USA) supplemented with B27 (1:50, Gibco), basic fibroblast growth factor (bFGF) and epidermal growth factor (EGF) (20 ng/mL each; Sigma-Aldrich), and 1% penicillin-streptomycin. Cultivation occurred in ultra-low attachment flasks (Corning) to promote neurosphere formation. The GSC spheres were periodically dissociated using Accutase solution (Gibco, USA). The stemness of the isolated GSCs was validated and maintained as described in prior research.[21] For the sphere formation assay, the transduced cells were seeded at a density of 5000 cells per well in ultra-low attachment cell culture plates (6-well plates) and cultured for 2–3 weeks. The number and size of spheres were subsequently analyzed under a microscope. Sphere Formation Efficiency (SFE) was calculated as the percentage of spheres larger than 75 μm relative to the total number of cells initially inoculated.

Cell Lines

The cell lines U87 (RRID:CVCL_0022), U251 (RRID:CVCL_0021), U118 (RRID:CVCL_0633), and T98G (RRID: CVCL_0556) were acquired from the American Type Culture Collection (Gaithersburg, MD, USA). Similarly, the HA1800 cell lines (IMMO BIOTCH, Cat# IM-H437) were procured from the IMMOCEEL Cell Resource Platform. These cell lines were cultured in DMEM (Gibco, USA) supplemented with 10% FBS (Invitrogen, China) and 1% penicillin/streptomycin (Gibco, USA). All cells were maintained in a humidified incubator at 37°C with 5% CO_2.

Isolation and Characterization of GaMSC-Exos

GaMSCs lines were established and maintained following previously described protocols.[14,22] The three groups of GaMSCs (GaMSC-1,GaMSC-2 and GaMSC-3) were derived from fresh tumor tissues of three patients diagnosed with malignant glioma. For the isolation of GaMSC-derived exosomes (GaMSC-Exos), the GaMSCs were cultured in 10 cm Petri dishes until they reached 80–90% confluence. Subsequently, these GaMSCs were cultured in MSC-Exosome-depleted FBS medium (Exosome Depleted Fetal Bovine Serum, VivaCell Biosciences) for 48h, which we called the conditioned medium from the glioma-associated mesenchymal stromal/stem cells (GaMSCs-CM). GaMSCs-CM was subjected to ultracentrifugation at 100,000 g for 2 hours at 4°C to isolate the exosomes. All procedures were performed in strict adherence to aseptic techniques and standardized exosomal ultracentrifugation protocols. To verify the purity and identity of the isolated exosomes, Western blot analysis was conducted using classical exosomal surface markers CD9, CD63, and CD81. Calnexin served as a negative control to confirm the absence of non-exosomal proteins. Additionally, the Flow NanoAnalyzer (NanoFCM) was employed to further characterize the surface markers (CD9, CD63, and CD81). The morphology of the exosomes was examined using transmission electron microscopy (TEM). A 20 μL sample of the exosome suspension was placed on 200-mesh grids and allowed to settle for 10 minutes at room temperature. The grids were then negatively stained with 2% phosphotungstic acid for 3 minutes, and excess liquid was carefully removed with filter paper before examination using an HT7800 transmission electron microscope. Furthermore, nanoparticle tracking analysis (NTA) was utilized to determine the particle size and concentration of the exosomes. The internalization of GaMSC-Exos was meticulously labeled with PKH26, and the uptake by target cells was visualized using the Olympus FV3000 confocal fluorescence microscope (Olympus Corporation, Japan).

Total RNA Extraction and Real-Time Quantitative PCR

Total RNA was extracted from fresh tissues and cells utilizing TRIzol Reagent (Invitrogen) in accordance with the manufacturer's instructions. MiRNA was reverse-transcribed into cDNA using the miRNA 1 Strand cDNA Synthesis Kit (AG11716, ACCURATE, China). This process involved the miRNA RT Enzyme Mix and 2X miRNA RT Reaction

Solution, and was conducted at 37°C for 1 hour followed by 85°C for 5 minutes. Subsequent RT-qPCR of the cDNA was performed employing the SYBR® Green Premix Pro Taq HS qPCR Kit II (AG11702, ACCURATE, China). The PCR protocol included an initial denaturation at 95°C for 30 seconds, followed by 40 cycles of 95°C for 5 seconds and 60°C for 20 seconds. Additionally, the Evo M-MLV One Step RT-qPCR Kit (SYBR) (AG11732, ACCURATE, China) facilitated simultaneous mRNA reverse transcription and RT-qPCR in a single tube, under conditions of 5 minutes at 42°C and 10 seconds at 95°C, followed by 40 cycles of 95°C for 5 seconds and 60°C for 30 seconds. U6 served as the endogenous control for miR-191-5p, while GAPDH was the internal control for other genes. Primer sequences for these genes are detailed in Supplementary Table S2, provided by Accurate Biology.

miRNA Sequencing and Cell Transfection

Total RNA from exosomes and their parental cells was extracted using the TRIzol reagent (Invitrogen, USA). Small RNA sequencing libraries were prepared using the TruSeq Small RNA Sample Prep Kits and were sequenced on the Illumina HiSeq 2000/2500 platform with a read length of 50 bp.

For cell transfection, PTEN plasmids, miRNA-191-5p mimics or miR-control mimics, and miRNA-191-5p inhibitors or miR-control inhibitors (Genomeditech, Wuhan) were introduced into glioma cells via Lipofectamine 3000 (Invitrogen), following the manufacturer's guidelines. Transfection efficiencies were assessed 48 hours post-transfection by RT-qPCR or Western blotting, after which the cells were used for subsequent experiments. The sequences of the RNA oligonucleotides used in these experiments are listed in Supplementary Table S3.

Tumorigenicity of Glioma Cells in vitro

The viability of glioma cells was evaluated utilizing the Cell Counting Kit-8 (CCK-8, MedChemExpress, China). Glioma cells were plated at a density of 1×10^4 cells per well in a 96-well plate and maintained in DMEM supplemented with 10% exosome-depleted fetal bovine serum (Gibco, USA) or GaMSCs-CM. To this culture, 1×10^5 exosomes were added every 24 hours, and a 10 μL aliquot of CCK8 solution was introduced at 24, 48, 72, and 96 hours post-seeding. The optical density at 450 nm was then measured using a microplate reader (PerkinElmer, USA).

A wound healing assay was conducted to assess the migratory capacity of the glioma cells. Cells were cultured in 6-well plates at a density of 1×10^6 cells per well until reaching approximately 90% confluence. Perpendicular scratches were then created using a 200-μL pipette tip, after which the medium was replaced with either serum-free DMEM or serum-free GaMSCs-conditioned medium, with or without 1×10^5 exosomes/μL. The gap width of the scratch wounds was recorded at 0 and 24 hours using an Olympus IX73 inverted microscope (Olympus, Japan).

To evaluate invasive capabilities, a Transwell assay (Corning Transwell® 24-well Permeable Support, 8μm) was utilized. The lower chambers were filled with 700 μL of DMEM containing 10% exosome-depleted fetal bovine serum (Procell, China) or GaMSCs-conditioned medium. After 24 hours of serum starvation, glioma cells (1×10^4 cells per well) subjected to various treatments were resuspended in 100 μL of serum-free medium and seeded into the upper chamber. Following a 24-hour incubation period, cells within the inserts were fixed with 4% paraformaldehyde and stained using a crystal violet solution. Imaging and cell counting were performed using an Olympus IX73 inverted microscope (Olympus, Japan) and analyzed with ImageJ software.

Immunofluorescence and Immunohistochemistry

Various glioma cell types (1×10^5 cells/well) were cultured in 24-well plates, fixed in 4% paraformaldehyde, and treated with 0.1% Triton X-100. The cells were subsequently incubated with 10% donkey serum at room temperature for 30 minutes. Following this, they were incubated with primary antibodies overnight at 4°C. AlexaFluor 488-conjugated donkey anti-mouse antibody was then applied and allowed to incubate at 37°C for 45 minutes. FITC-Phalloidin (1:200) and DAPI solution were added and the cells were incubated in darkness for 5 minutes. After mounting with anti-fade medium, the cells were visualized using an Olympus IX73 inverted microscope (Olympus, Japan). For immunofluorescence, GSC spheres were seeded onto poly-L-lysine coated glass slides (30 μg/mL) at a density of 10,000 cells/ cm^2 to facilitate adhesion. The spheres were then fixed, permeabilized, and incubated overnight at 4°C with primary antibodies (Ki67, 1:100; Sox2, 1:100; Vimentin, 1:2000).

After washing with PBS, the spheres were treated with AlexaFluor 488 or AlexaFluor 647-conjugated donkey anti-mouse antibodies. The subsequent steps were identical to those described previously.

Tumor tissues were initially preserved in 4% paraformaldehyde, embedded in paraffin, and sectioned into 4-μm slices. These sections were deparaffinized using xylene and ethanol to remove paraffin residues. A blocking step with 5% normal goat serum was performed before the slices were incubated overnight at 4°C with primary antibodies (anti-PTEN, 1:500; anti-Sox2, 1:100; anti-Vimentin, 1:5000; anti-Akt, 1:300; anti-Phospho-Akt, 1:100; anti-Ki67, 1:2000). Subsequently, the sections were exposed to an HRP-conjugated secondary antibody and streptavidin-peroxidase (1:200). The average integral optical density of positively stained slides was quantified using ImageJ software version 1.54b (National Institutes of Health).

Dual-Luciferase Reporter Assay

The JASPAR database (https://jaspar.genereg.net/) was utilized to predict potential miR-191-5p binding sites within the PTEN sequence. Subsequently, dual luciferase reporter gene vectors, pGL6-miR-PTEN-3`UTR-WT and pGL6-miR-PTEN-3`UTR-Mut (Genomeditech, Wuhan), were constructed. PTEN-3`UTR-WT or PTEN-3`UTR-Mut reporter plasmids were co-transfected with miR-191-5p mimics or control miR-mimics (Genomeditech, Wuhan), along with the pRL-TK Renilla luciferase plasmid into U87 cells using Lipofectamine 3000 (Invitrogen, China) as the transfection reagent. The pRL-TK Renilla luciferase plasmid served as an internal control to normalize for transfection efficiency. After 24 hours, the cellular supernatant was collected, and luciferase activity was measured using the Dual-Luciferase® Reporter Assay System (Beyotime Biotechnology, China). Firefly and Renilla luciferase activities were detected sequentially using a luminometer. The relative luciferase activity was calculated by dividing the firefly luciferase signal by the Renilla luciferase signal (FLuc/RLuc). All values were normalized to the control group, and experiments were performed in triplicate with at least three independent repeats.

Western Blotting

Total protein was extracted from cells or tissues using RIPA buffer supplemented with 1 mM PMSF (Beyotime). The proteins were separated on a 4–12% FuturePAGE™ Protein Precast Gel (ACE Biotechnology, China) and subsequently transferred onto a polyvinylidene fluoride (PVDF) membrane. Visualization of protein bands was facilitated using a Thermo Scientific PageRuler (26616). The membrane was blocked with 5% nonfat milk. It was then incubated overnight at 4°C with the following primary antibodies: PTEN (1:1000), Sox2 (1:1000), Vimentin (1:20,000), CD44 (1:20,000), GAPDH (1:50,000), Phospho-Akt (1:1000), Akt (1:1000), and Olig2 (1:1000). This was followed by incubation with horseradish peroxidase-conjugated secondary antibodies at 37°C for 1.5 hours. Band intensities were visualized using an enhanced Common ECL chemiluminescence kit (G2014, Servicebio, China) and detected with a Bio-Rad imaging system (Hercules, CA, USA). GAPDH was used as a loading control to normalize the density of each protein band. Details of all antibodies and their corresponding item numbers are listed in Supplementary Table S4.

Microarray Analysis

Glioma microarray datasets were retrieved from the Gene Expression Omnibus (GEO) database (https://www.ncbi.nlm.nih.gov/geo/), analyzing datasets GSE139031 and GSE90603 using the R programming language. The CGGA database (http://www.cgga.org.cn/index.jsp) was employed to validate the relationship between miRNA expression and glioma grade, in addition to conducting survival analyses. Gene Ontology (GO) enrichment analysis was performed using KOBAS 3.0 from the Gene-list Enrichment database (http://kobas.cbi.pku.edu.cn/index.php).

DAB-In Situ Hybridization (ISH)

The miRNA-191-5p probe (5′-CAGCTGCTTTTGGGATTCCGTTG-3′) was custom-synthesized by Servicebio Technology CO., Ltd. ISH was conducted according to the manufacturer's instructions for in situ hybridization reagents (Servicebio, Wuhan, China).[23] Tissues were washed with PBS and fixed in an in-situ hybridization fixative (G1113, Servicebio, China) for over 12 hours. Paraffin-embedded sections were then incubated with a hybridization solution (G3045, Servicebio, China) containing the probes at 54°C overnight.

Following hybridization, a branch probe was used as an intermediary to enhance the binding of additional signal probes, amplifying the signal. An HRP-labeled anti-digoxin antibody (200–032-156, Jackson) was used to bind the digoxin-labeled nucleic acid hybrids. DAB staining (DAB kit, G1212, Servicebio, China) was applied for 5 minutes at room temperature, and nuclei were stained with hematoxylin for 2.5 minutes at room temperature. This staining produced an insoluble brownish-yellow product, allowing for the localization and quantification of the target gene-probe hybrid. The main criterion for interpreting the results was that the nuclei stained with hematoxylin appeared blue, while DAB-positive expression appeared brownish yellow under a white light microscope (Olympus IX73 inverted microscope, Japan).

Tumor-Bearing Mice

Female BALB/c mice, aged 4 weeks and weighing 18–21 grams, were acquired from Hubei Biont Biological Technology Co., Ltd. The mice were accommodated in the SPF animal experiment center at Tongji Medical College, Huazhong University of Science and Technology. Conditions maintained included a room temperature of $22\pm2°C$, humidity of 55 $\pm5\%$, and a 12-hour light/dark cycle. The mice had unrestricted access to food and water. GSCs underwent retroviral transduction employing the Pinco-pGL3-luc/GFP vector, which encodes firefly luciferase (FFL), as described in previous studies.[24] Cells expressing green fluorescent protein (GFP) were isolated using a FACS Aria II cell sorter (BD Biosciences, San Jose, CA). Isoflurane was employed to anaesthetize the mice. The luciferase-labeled GSCs were pre-treated with exosomes (1×10^9 exosomes/μL), miRNA-191-5p agomir/antagomir, or NC from Genomeditech, China, for 24 hours. All mice were anesthetized with isoflurane inhalation prior to each injection. Subsequently, the treated GSCs (5×10^6 cells) were injected into the right frontal lobe. Exosomes (1×10^9 exosomes/mL) derived from GaMSCs were administered intratumorally five times at 3-day intervals. miRNA-191-5p agomir/antagomir or NC from RiboBio, China, was directly injected into the implanted tumor every 5 days. Tumor progression was monitored and evaluated using bioluminescence imaging (PerkinElmer, IVIS Spectrum Imaging System). After a period of 25 days, each mouse was rapidly anesthetized with isoflurane, decapitated, and their tumor tissues were harvested for further analysis. The animal study adhered to ethical standards and received approval from the Experimental Animal Ethics Committee of Huazhong University of Science and Technology (IACUC Number: 3854). All procedures conformed to the Chinese Law on Laboratory Animal Welfare (Guideline for Ethical Review of Animal Welfare, Standard number: GB/T 35892–2018). The sequences of miRNA-191-5p agomir/antagomir or NC are presented in Supplementary Table S3.

Statistical Analysis

Statistical data were analyzed using SPSS 22.0 software or GraphPad Prism v9.0, and expressed as the mean ± standard deviation from three independent experiments. For comparisons between two groups, an unpaired two-tailed Student's t-test or a paired two-tailed Student's t-test was utilized. For multiple comparisons, a one-way analysis of variance (ANOVA) with Dunnett's post-hoc test was employed. The Kaplan–Meier method was used to assess the overall survival rate among patients. Pearson's correlation analysis, applicable to normally distributed data, was performed to examine the associations between miR-191-5p and PTEN, ensuring both variables approximately conformed to a normal distribution.

Results
Isolation and Characterization of GaMSC-Exos

In Our Study, Three Groups of GaMSCs (GaMSC-1,GaMSC-2, GaMSC-3) Were isolated from human glioma surgical specimens and subsequently utilized for exosome isolation (Figure 1A). These cell lines exhibited classical characteristics of mesenchymal stromal/stem cells, including high expression levels of CD105, CD73, and CD90, and low expression of CD31 (Figure 1B). Additionally, these GaMSCs demonstrated the capacity to differentiate into osteoblasts, adipocytes, and chondroblasts under specific in vitro stimuli (Figure 1C). Differentiation was confirmed using Oil Red O, Alizarin Red, and Alcian Blue staining techniques for adipogenic, osteogenic, and chondrogenic differentiation, respectively.

Exosomes secreted by these GaMSCs lines were isolated from the supernatant of the GaMSCs conditioned medium (GaMSCs-CM) by ultrafast centrifugation method. Transmission electron microscopy (TEM) revealed the bilayer membrane ultrastructure typical of exosomes and their characteristic sizes (Figure 1D). Nanoparticle tracking analysis

(NTA) showed that these exosome particles ranged in diameter from 40 to 150 nm, with concentrations of 3.5–4.5E+6 particles/mL (Figure 1E). Flow NanoAnalyzer analysis indicated that the GaMSC-Exos expressed typical exosomal markers CD9, CD63, and CD81 (Figure 1F). Western blot analysis confirmed the presence of these markers on the surface of GaMSC-Exos, while calnexin, an endoplasmic reticulum marker, was absent (Figure S1E). Consequently, GaMSC-Exos are likely secreted from GaMSCs into the microenvironment and may play a role in cell-cell communication within glioblastoma.

GaMSC-Exos Promote PMT of Glioma Cells as a Key Messenger

To explore the interactions between GaMSCs and glioma cells, we initially employed GaMSCs-CM to evaluate its impact on glioma cell tumorigenicity. The conditioning of glioma cells with GaMSCs-CM significantly enhanced their proliferation, migration, and invasion capabilities, as demonstrated in CCK-8 assays (fold change >1.5, $P < 0.0001$), Wound healing
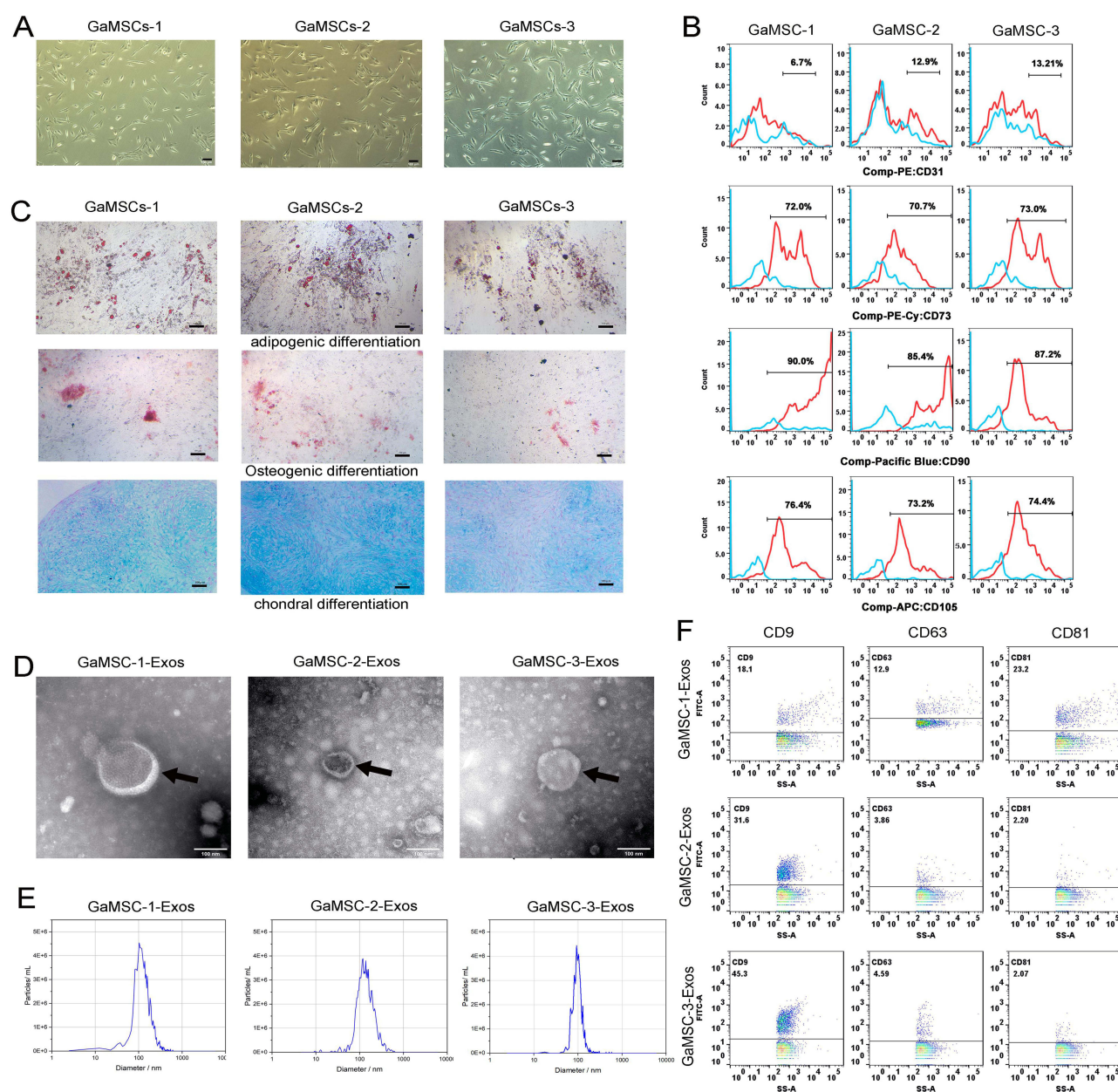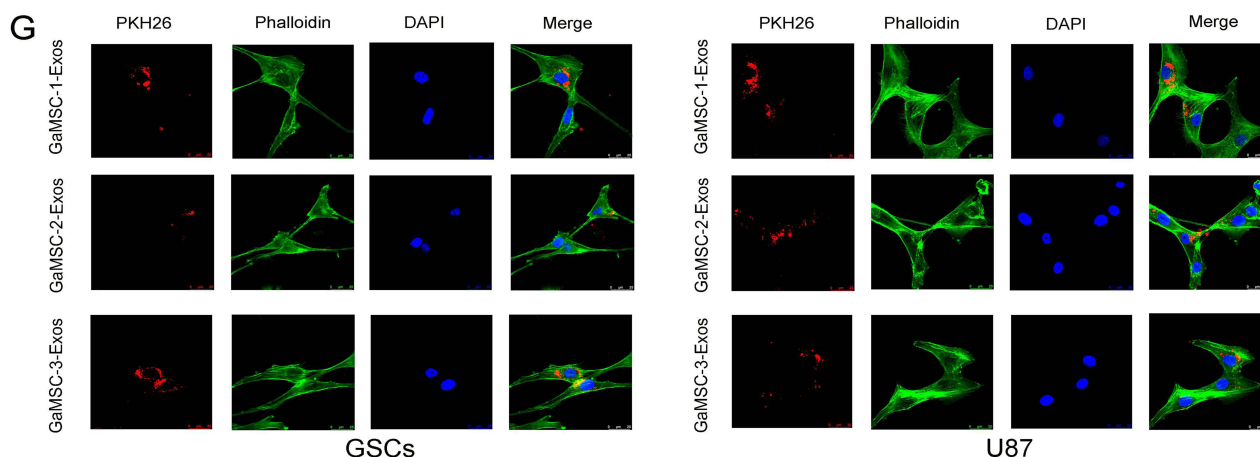

Figure 1 Continued.

Figure 1 Characterization of GaMSCs and Identification of GaMSCs-Exos. (**A**) GaMSCs exhibit a flat fusiform shape in MSC medium (scale bars = 100 μm). (**B**) Flow cytometric analysis confirmed the presence of MSC markers (CD31, CD105, CD73, and CD90) in GaMSCs lines cultured in vitro. (**C**) Three groups of GaMSCs lines successfully differentiated into osteoblasts, adipocytes and chondrocytes (scale bars = 100 μm). (**D**) Transmission electron microscopy (TEM) was employed to image three groups of GaMSCs-Exos (scale bar = 100 nm). The black arrows indicate the exosomes. (**E**) Nanoparticle Tracking Analysis (NTA) measured the size and concentration of three groups of GaMSC-Exos. (**F**) Flow NanoAnalyzer analysis the surface markers of GaMSC-Exos (CD9,CD63 and CD81). (**G**) Absorption of GaMSC-Exos by GSCs and U87 was visualized; PKH26-labeled exosomes appeared red, glioma cells stained with 488-Phalloidin were green, and nuclei stained with DAPI were blue (scale bar = 25 μm).

assays (fold change >2.50, P < 0.0001), and Transwell assays (fold change >2.0, P < 0.0001, Figure S1A–C). Following this observation, we isolated exosomes from GaMSCs-CM and used them to stimulate glioma cells in order to determine whether the exosomes exerted similar effects.

To investigate the role of GaMSC-Exos within the TME, three GaMSC-Exos samples were collected and subsequently co-cultured with glioma cell lines (U87 and U251) and GSCs for 12 hours. A significant uptake of PKH26-labeled exosomes, exhibiting red fluorescence, was observed within the cytoplasm of glioma cells via confocal microscopy, indicating phagocytosis of these exosomes (Figures 1G and S1D). When conditioned with GaMSC-Exos, glioma cells demonstrated enhanced proliferation, migration, and invasion capabilities, as depicted in Figure 2A–C.

PMT has been identified as a crucial phenotypic adaptation, significantly contributing to the maintenance of tumorigenic behaviors in glioblastoma. Recent studies suggest that alterations in cytoskeletal status are critical in PMT.[25] Vimentin, a major cytoskeletal component and a recognized marker of metastasis was assessed to explore the influence of GaMSC-Exos on PMT progression.[26] After 48 hours of treatment with GaMSC-Exos, immunofluorescence analysis revealed increased perinuclear and nuclear localization of the MES marker Vimentin in U87 and U251 cells (fold change >1.5, p < 0.0001, Figure 2D). Western blot analysis further confirmed that GaMSC-Exos significantly upregulated Vimentin expression in these glioma cells (Figure S2).

Additionally, the impact of GaMSC-Exos on GSCs' self-renewal was investigated through tumorsphere formation assays. Compared with the control group, GaMSC-Exos substantially increased the SFE (fold change > 2.0, P < 0.05) and the diameter of tumorspheres (fold change > 2.0, P < 0.05, Figure 3A). These results suggest that GaMSCs could promote malignant tumorigenic behaviors of glioma cells through the secretion of GaMSC-Exos.

Further analyses were conducted on the expression and localization of the MES marker Vimentin, the PN marker Sox2, and the proliferative marker Ki67 in GSC tumorspheres. The expression levels of Ki67 and Vimentin were elevated, whereas Sox2 expression decreased (Figure 3B). Western blot results demonstrated significant upregulation of CD44 and Vimentin, alongside downregulation of Olig2 and Sox2, in glioma cells conditioned with GaMSC-Exos compared to the control group (Figure S2). These findings indicate that GaMSCs secrete exosomes to promote PMT, thereby enhancing the tumorigenicity of glioblastoma cells in vitro.

To assess the role of GaMSC-Exos in PMT in vivo, 5×10^5 luciferase-labeled GSCs pretreated with GaMSC-Exos were injected into the right frontal lobe of nude mice. Compared with the control group, xenografts regularly injected with GaMSC-Exos (1×10^9 exosomes/mL, five times every three days) displayed significant tumor growth enhancement 25 days post-implantation (fold change > 2.0, P < 0.05, Figure 3C–E). IHC results revealed that GaMSC-Exos treatment

led to a considerable increase in tumor volume and induced upregulation of Vimentin and downregulation of Sox2 compared to the control group (Figure 3F and G, fold change > 1.5, P < 0.05). Additionally, Ki-67 expression was significantly enhanced following GaMSC-Exos treatment (fold change > 1.5, P < 0.05). These findings further corroborate that GaMSC-Exos facilitate PMT of glioma cells, enhancing their tumorigenic potential.

The Impact of GaMSC-Exos on Glioma Cells Mediated by Exosomal miRNA-191-5p

Exosomes have been identified as vehicles for the delivery of miRNAs to target cells, facilitating cell-to-cell communication within the tumor microenvironment.[1,18,27] In this study, we examined the miRNA expression profiles in GaMSCs lines and GaMSC-Exos using next-generation sequencing (see Figure 4A). Venn diagram analysis identified an overlap of 141 miRNAs across three microarray datasets of exosomes (Figure 4B). Further analysis of these 141 miRNAs, focusing on the top 50 most abundantly expressed, revealed that miRNA-191-5p was particularly elevated in the exosomal miRNAs (Figure 4C).

Our preliminary experiments demonstrated that certain highly expressed miRNAs, (e.g.hsa-let-7, hsa-miR-29, and hsa-miR-22.etc). inhibited tumor proliferation. Conversely, others including hsa-miR-21, hsa-miR-27, and hsa-miR-221, were implicated in promoting epithelial-to-mesenchymal transition (EMT) in glioma. Notably, miRNA-191-5p was identified as a specific promoter of PMT. Additionally, miRNA-191-5p exhibited significantly higher expression levels
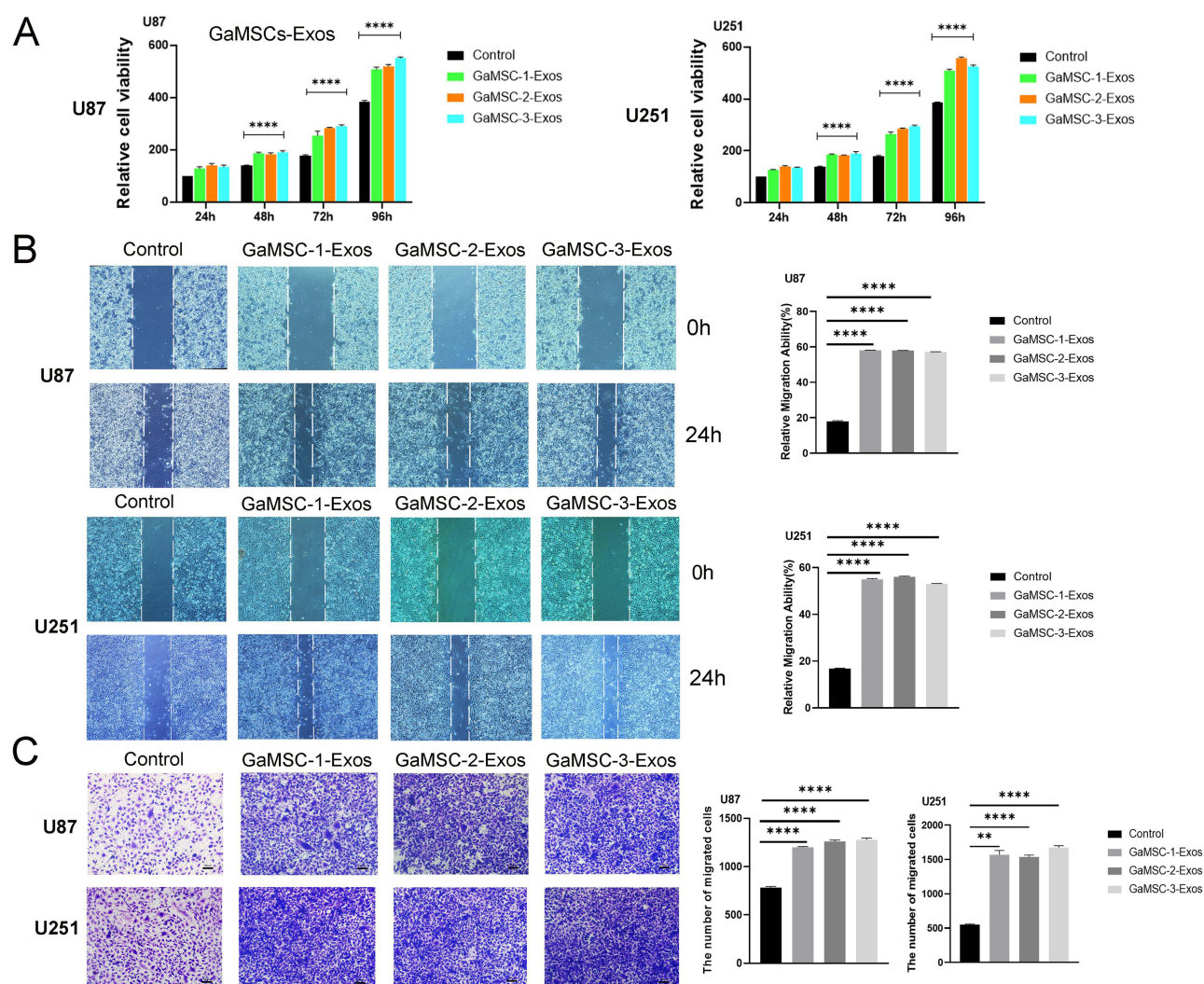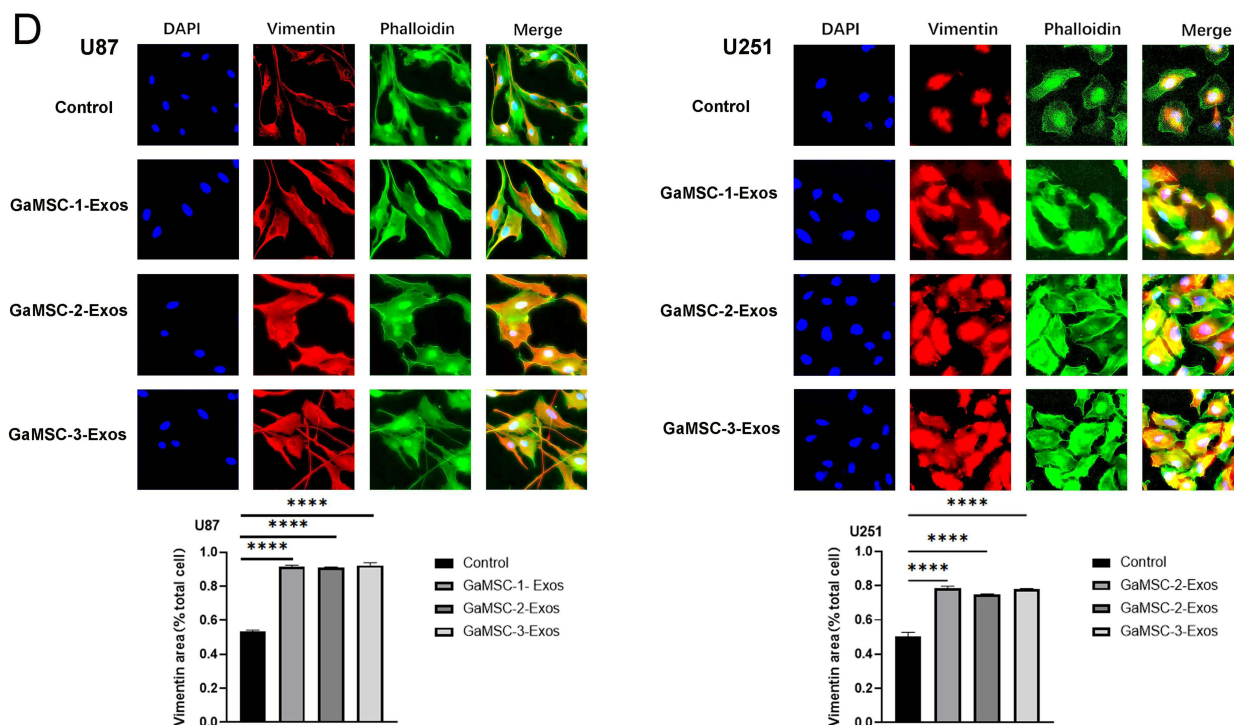

Figure 2 Continued.

Figure 2 GaMSCs-Exos Enhanced Proliferation, Invasion, and Mesenchymal Subtype Formation in U87 and U251 Cells (**A**) CCK-8 assays show enhanced proliferation in U251 and U87 cells cultured with GaMSCs-Exos; significant increase compared to control (****P < 0.0001). (**B**) Wound healing assays indicate increased migration in U251 and U87 cells treated with GaMSCs-Exos; significant improvement compared to control (****P < 0.0001). (**C**) Transwell assays reveal a marked increase in the invasiveness of U251 and U87 cells cultured with GaMSCs-Exos (**P < 0.01; ****P < 0.0001; scale bar = 100 μm); (**D**) Immunocytochemistry confirmed increased vimentin expression and its subcellular localization in U87 and U251 cells treated with GaMSCs-Exos. Quantification of the vimentin area proportions (%) of the cells cultured with GaMSCs-Exos using ImageJ; substantial elevation compared to control (****P < 0.0001, scale bar = 200 μm). Data represent mean ± SEM from three independent experiments; statistical significance assessed using two-tailed Student's t-tests or one-way ANOVA followed by Dunnett's test for multiple comparisons: **P < 0.01; ****P < 0.0001.

in GaMSC-Exos compared to GaMSCs alone (fold change > 1.5, P < 0.001, Figure 4D). The expression levels of miRNA-191-5p in GSCs and U87 and U251 cell lines substantially increased following treatment with GaMSC-Exos (fold change > 1.5, P < 0.001, Figure 4E).

The differential expression of miRNA-191-5p was further investigated in glioma tissues compared to normal brain tissue using data from the GEO database (GSE139031 and GSE90603, Figure 4F and G). The results indicated a significantly higher expression level in glioma tissues (p < 2e-16 and p = 0.00019, respectively). Moreover, a positive correlation was observed between miRNA-191-5p expression levels, high-grade glioma, and poorer survival outcomes, as indicated by analysis of the Cancer Genome Atlas (CGGA) database (Figure 4H and I, P < 0.05).

The involvement of miRNA-191-5p in cancer-related signaling pathways was confirmed using the KOBAS 3.0 Gene-list Enrichment database (http://kobas.cbi.pku.edu.cn/index.php), where it was found to be significantly enriched in the MicroRNA of cancers signaling pathway (Figure 4J). Additionally, the expression levels of miR-191-5p were quantified in various glioma cell lines (GSCs, U251, U87, U118, and T98G) and in normal neuroglial cells (HA1800) using RT-qPCR (Figure 4K). Subsequently, GSCs, U87 and U251 were selected for further tests.

miRNA-191-5p Promotes Tumorigenicity and Proneural-to-Mesenchymal Transition in Glioma Cells

To elucidate the role of miRNA-191-5p in glioblastoma in vitro, we manipulated its expression in glioblastoma cells and monitored various cellular processes. Our results demonstrated that overexpression of miRNA-191-5p in U87 and U251 cells significantly enhanced proliferation (p < 0.0001), migration (fold change > 2.0, p < 0.0001), and invasion (fold change > 2.0, p < 0.0001) of glioma cells. Conversely, inhibition of miRNA-191-5p expression diminished these capabilities (p < 0.0001;
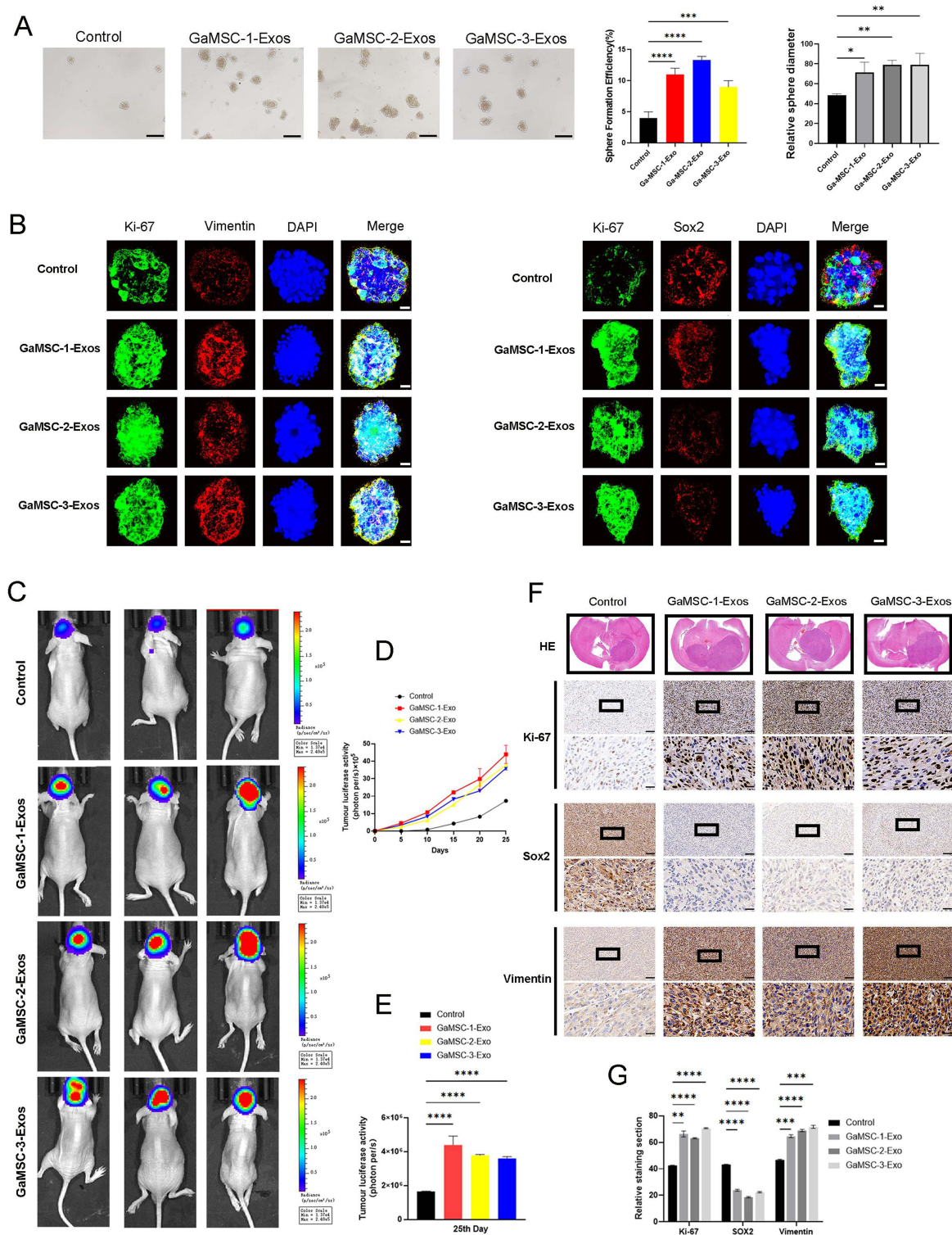
Figure 3 GaMSCs-Exos Promote Tumorigenicity and Formation of Mesenchymal Glioblastoma Subtypes in GSCs. (**A**) Bright field microscopy revealed enhanced sphere formation in GSCs treated with GaMSCs-Exos compared to control. Left: statistics of sphere counts; right: quantification of sphere diameters (scale bar = 200 μm). (**B**) Immunofluorescence images depict Vimentin/Sox2 in red and Ki-67 in green expression in GSCs treated with GaMSCs-Exos. Nuclei were counterstained with DAPI (blue) (scale bar = 25 μm). (**C**) Bioluminescent imaging tracked intracranial tumor growth in xenograft nude mice bearing luciferase-expressing GSCs treated with GaMSCs-Exos and control on day 25. Intensity of bioluminescence is represented on a color scale (photons/s/cm²/steradian); n = 3. (**D**) Bioluminescent images were recorded every 5 days to monitor tumor growth dynamics. (**E**) Histogram analysis quantified the luminescence indicating tumor size on day 25. (**F**) Representative images of H&E staining show histological features (scale bar = 1 mm, n=3), and IHC staining demonstrates Ki67, Sox2, and Vimentin expression (upper panels, scale bar = 100 μm; lower panels, scale bar = 25 μm, n=3) in intracranial xenografts. (**G**) Histogram analysis presents relative expression levels of Ki67, Vimentin, and Sox2 in xenograft tissues. Data represent mean ± SEM from three independent experiments; statistical significance determined by two-tailed Student's t-tests or one-way ANOVA followed by Dunnett's tests for multiple comparisons: *P < 0.05; **P < 0.01; ***P < 0.001; ****P < 0.0001.
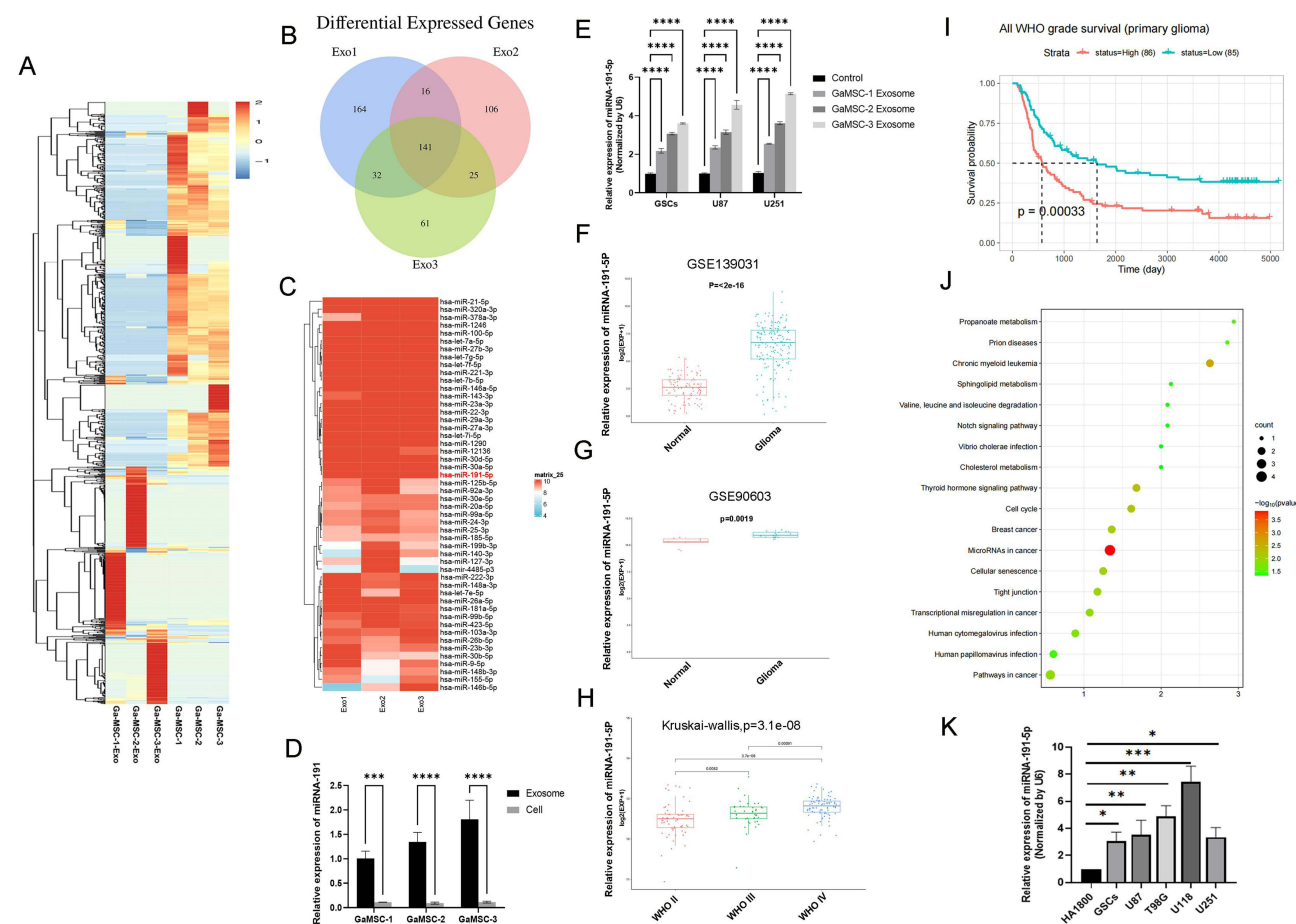
Figure 4 Elevated Expression of miRNA-191-5p in GaMSCs-Exos. (**A**) A heatmap displays differentially expressed miRNAs in exosomes from three groups of Ga-MSCs lines and GaMSCs-Exos, analyzed using deep sequencing on the ACGT101-miR(v4.2) platform. (**B**) Venn diagram showing the intersection of the top 141 miRNAs common to three groups of GaMSCs-Exos. (**C**) A heatmap illustrates the intersection of the top 50 miRNAs across three groups of GaMSCs-Exos. Red text indicates significantly upregulated miRNAs. (**D**) Expression levels of miRNA-191-5p in three groups of GaMSCs-Exos and GaMSCs, quantified by RT-qPCR. (**E**) Increased levels of miRNA-191-5p in GSCs, U87, and U251 cells treated with GaMSCs-Exos compared to control, as determined by RT-qPCR. (**F**) (**G**) Analysis of miRNA-191-5P expression in normal and glioma samples from datasets GSE139031 and GSE90603; blue represents normal samples, red represents glioma samples. (**H**) The expression of miRNA-191-5p across different glioma grades in the CGGA database; red indicates WHO grade II, green WHO grade III, and blue WHO grade IV glioma samples. (**I**) Kaplan-Meier survival curves compare overall survival in primary glioma patients with high versus low expression of miRNA-191-5p in the CGGA database; low expression correlates with longer survival (P = 0.00033). Survival analysis utilized the Log rank test. (**J**) KEGG pathway enrichment analysis of miRNA-191-5p conducted using Kobas 3.0. (**K**) Expression of miRNA-191-5p in glioma cell lines detected by RT-qPCR. GSCs, U251 and U87 was selected for follow-up tests. Data are presented as mean ± SEM from three independent experiments; statistical significance assessed by two-tailed Student's t-tests or one-way ANOVA followed by Dunnett's tests for multiple comparisons: *P < 0.05; **P < 0.01; ***P < 0.001; ****P < 0.0001.

Figure S3A–C). Additionally, the expression area of the mesenchymal marker Vimentin increased in the miRNA-191-5p mimic groups and decreased in the inhibitor groups compared to control groups (Figure S3D).

Overexpression of miRNA-191-5p also promoted SFE and increased the diameter of tumorspheres in GSCs, whereas knockdown of miRNA-191-5p inhibited this proliferative potential relative to that in the miR-Control mimics/inhibitor group (Figure 5A). Upregulation of miRNA-191-5p in GSC spheres led to increased expression of the proliferation marker Ki67 and Vimentin, and reduced expression of the proneural cell marker Sox2, compared to the miR-control groups. In contrast, inhibition of miRNA-191-5p reversed these effects in immunofluorescence analyses (Figure 5B). Western blot results confirmed a significant upregulation of CD44 and Vimentin, and a downregulation of Olig2 and Sox2 upon miRNA-191-5p overexpression. Suppression of miRNA-191-5p led to a decrease in CD44 and Vimentin expression and an increase in Olig2 and Sox2 levels (Figure S4).

In vivo, a xenograft tumor model in nude mice was utilized to assess the impact of miRNA-191-5p on the PMT of glioma. Intervention with miRNA-191-5p agomir significantly enhanced tumor growth compared to the control group (fold change > 2.0, p < 0.001), while administration of miRNA-191-5p antagomir suppressed tumor growth (fold
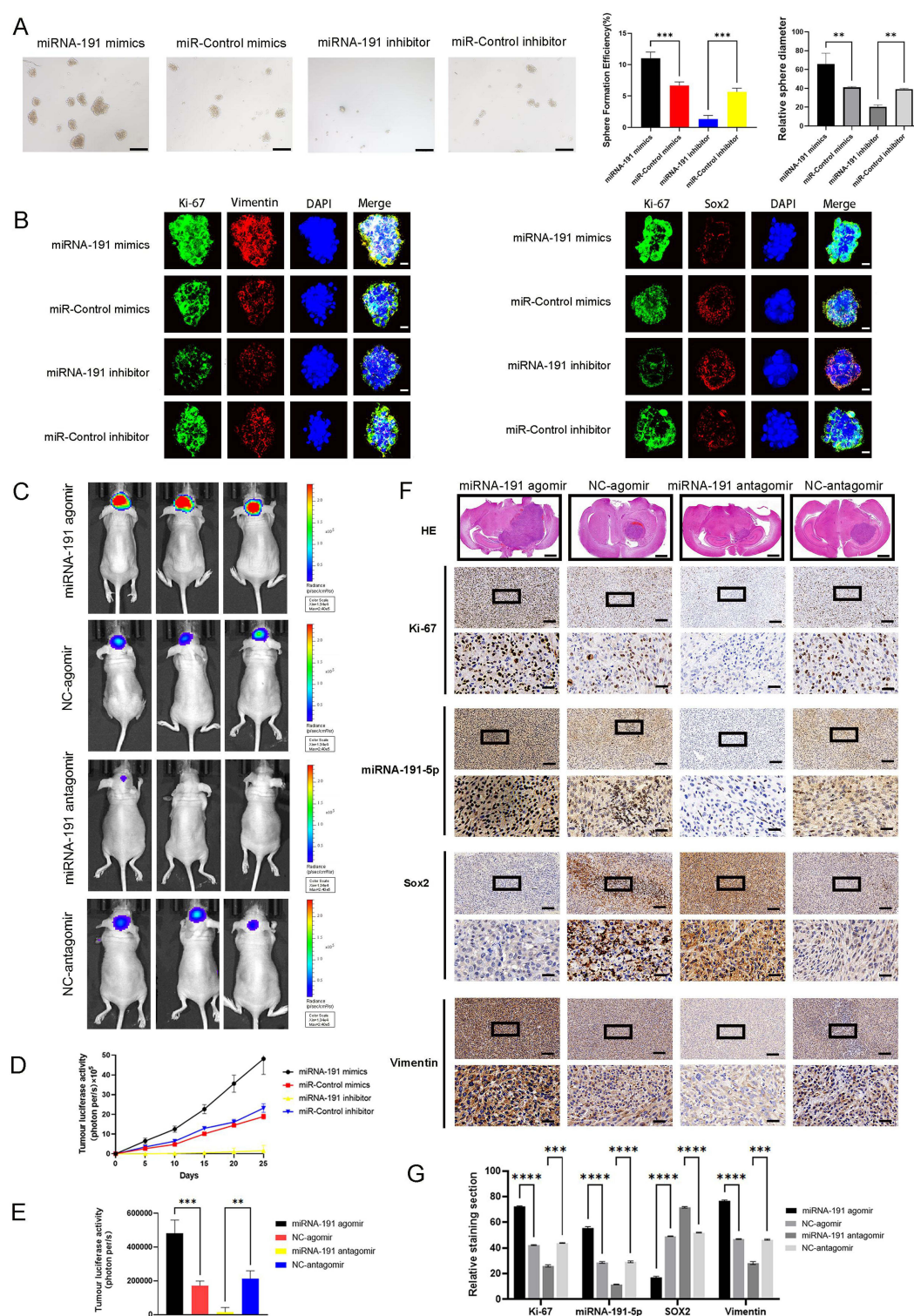
Figure 5 miRNA-191-5p Promoted The Tumorigenicity and PMT of Glioma Stem Cells. (**A**) Representative bright field microscopy images show neurosphere formation in GSCs treated with miRNA-191-5p mimics or miR-control mimics, and miRNA-191-5p inhibitor or miR-control inhibitor. Scale bar = 200 μm. Left: sphere formation statistics; right: sphere diameter quantification. (**B**) Immunofluorescence images illustrate Vimentin/Sox2 in red and Ki-67 in green in GSCs treated with miRNA-191-5p mimics or miR-control mimics, and miRNA-191-5p inhibitor or miR-control inhibitor. Nuclei were counterstained with DAPI (blue). Scale bar = 25 μm. (**C**) Bioluminescence imaging tracked tumor growth in xenograft nude mice injected with luciferase-labeled GSCs transfected with miR-191-5p agomir/antagomir or NC control on day 25; n = 3. (**D**) Bioluminescent images were measured every 5 days. (**E**) Histogram analysis quantified the luminescence indicating tumor size on day 25. (**F**) (**G**) Representative H&E staining images (scale bar = 1 mm, n = 3) and IHC staining for Ki67, miRNA-191-5p, Sox2, and Vimentin (upper panels, scale bar = 100 μm; lower panels, scale bar = 25 μm, n = 3) in GSC-bearing xenografts treated with miR-191-5p agomir/antagomir or NC control. Data represent mean ± SEM from three independent experiments; **P < 0.01; ***P < 0.001; ****P < 0.0001 according to two-tailed Student t tests used for two-group comparisons.

change > 1.5, p < 0.01; Figure 5C–E). Immunohistochemistry and in situ hybridization analysis showed that miRNA-191-5p agomir induced upregulation of Ki67, miRNA-191-5p, and Vimentin, and downregulation of Sox2 compared to the control group, while miRNA-191-5p antagomir exhibited the opposite trend (Figure 5F and G). Collectively, these findings indicate that miRNA-191-5p fosters PMT, a process associated with increased malignancy and cell invasion in glioblastoma.

PTEN Is a Direct Target of miRNA-191-5p in Glioma

To ascertain the downstream targets of exosomal miRNA-191-5p in glioma, we employed sequence alignments through the JASPAR database (https://jaspar.genereg.net/). The alignments indicated that miRNA-191-5p possesses a potential binding site within the 3′-UTR of PTEN mRNA, suggesting a direct regulatory interaction (Figure 6A). Dual-luciferase reporter assay results demonstrated that transfection with miRNA-191-5p mimics significantly reduced the luciferase activity of the pGL6-miR-PTEN-3′-UTR-WT construct, whereas it had no effect on the pGL6-miR-PTEN-3′-UTR-MUT construct (Figure 6B). This suggests a specific interaction between miRNA-191-5p and PTEN mRNA. Western blotting and RT-qPCR analyses further confirmed that overexpression of miR-191 led to decreased PTEN expression, and conversely, suppression of miRNA-191-5p resulted in increased PTEN expression (Figure 6C and D).

Subsequent analysis using Pearson's correlation coefficient revealed a negative correlation between PTEN and miRNA-191-5p expression levels across 40 glioma cases, as determined by RT-qPCR (Figure 6E). Moreover, IHC analysis of intracranial tumors in mice showed lower PTEN expression in tumors overexpressing miRNA-191-5p and higher expression in tumors with suppressed miRNA-191-5p, compared to controls treated with NC-agomir/antagomir (Figure 6F). Collectively, these findings indicate that PTEN is a potential target gene of miRNA-191-5p and functions as a tumor suppressor gene in glioma.

miRNA-191-5p Regulates PTEN Expression Levels in Glioma

In gain-of-function and loss-of-function experiments, glioma cells were co-transfected with miRNA-191-5p mimics and PTEN plasmid to elucidate the regulatory relationship between them. In GSCs tumorspheres, upregulation of PTEN led to decrease tumorsphere formation and downregulation of Ki67 and Vimentin, while Sox2 expression was upregulated. However, these effects were substantially diminished upon reintroducing miRNA-191-5p expression (Figure 7A and B).

Further, overexpression of PTEN was shown to inhibit the proliferation, migration, and invasion of glioma cells as assessed by CCK-8, Wound healing assays, and Transwell assays. Nevertheless, these inhibitory effects were notably reduced upon restoration of miRNA-191-5p expression (Figure 7C–E). Immunofluorescence staining of glioma cells demonstrated that PTEN decreased the expression area of Vimentin, with this inhibitory effect being mitigated by the concurrent overexpression of miR-191-5p (Figure S5). Overall, these results indicate that exosomal miR-191-5p directly targets PTEN in glioma and promotes the PMT of glioblastoma cells.

Exosomal miRNA-191-5p Activates the PI3K/Akt Signaling Pathway in Glioblastoma Cells

To explore the interrelationship among miRNA-191-5p, PTEN, and the PMT in glioma progression, we analyzed the expression levels of PMT markers in glioma cells transfected with PTEN plasmids and miRNA-191-5p mimics via Western blot analysis (Figure 8A).The results showed that increasing PTEN expression raised the protein levels of Olig2 and Sox2 while reducing Vimentin and CD44 levels, indicating PMT suppression. Conversely, boosting miRNA-191-5p had the opposite effect, which could be reversed with PTEN plasmids. We further examined whether miRNA-191-5p modulates the PI3K/Akt signaling pathway by targeting PTEN in gliomas. The results demonstrated a substantial decrease in the p-Akt/Akt ratio in the presence of PTEN plasmid, which was restored upon re-introduction of miRNA-191-5p (Figure 8A). In conclusion, the PI3K/Akt signaling pathway is activated by miRNA-191-5p through the downregulation of PTEN.

We collected tumor samples from GBM patients diagnosed pathologically and molecularly as either PN- or MES-subtype for immunohistochemical analysis, including five patients per group. The IHC analysis revealed elevated levels of miRNA-
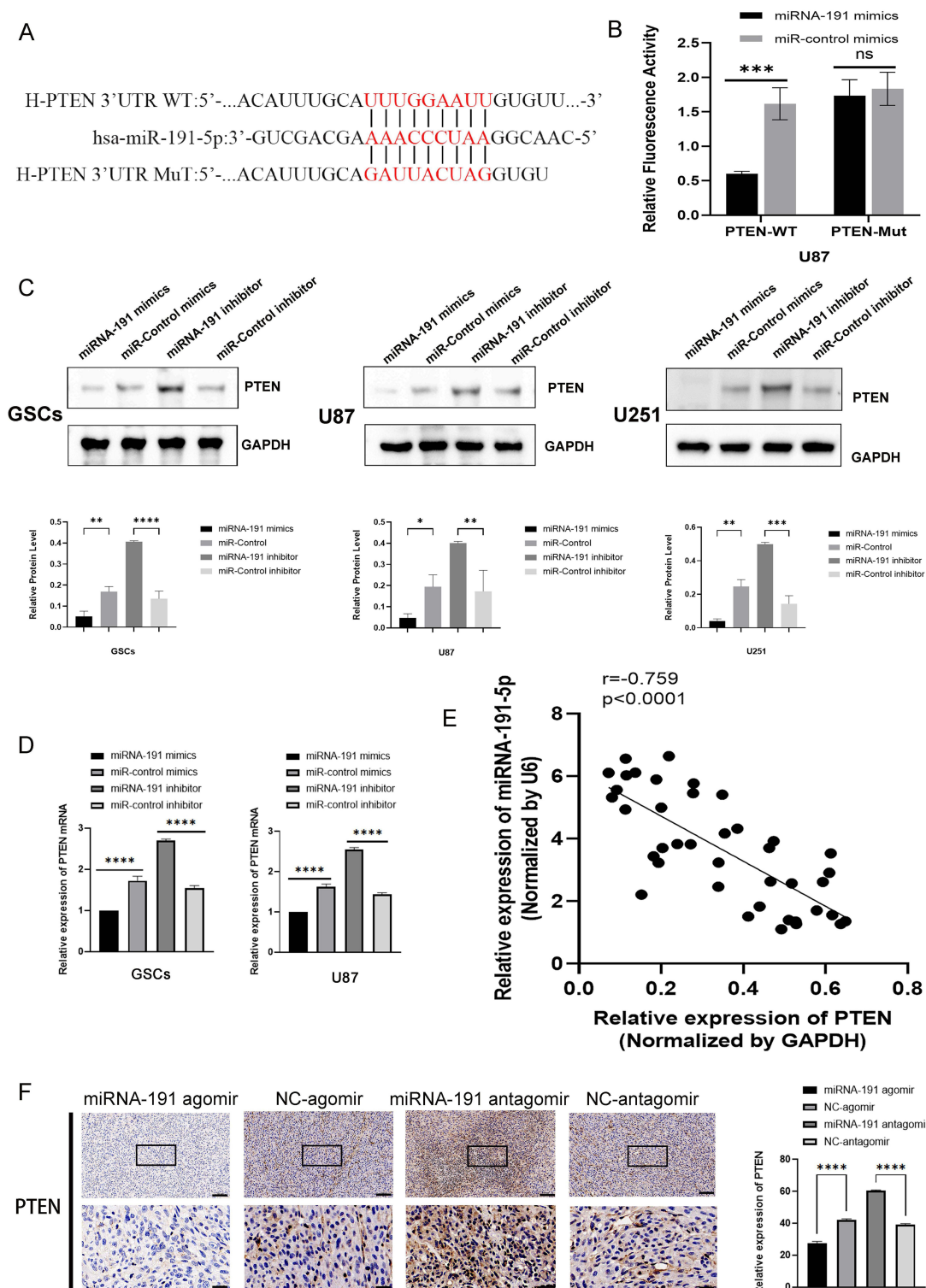
Figure 6 PTEN as a Direct Target of miRNA-191-5p in Glioma. (**A**) Sequence alignment illustrating potential binding sites between PTEN mRNA and miR-191-5p. The red text indicates the binding site between miR-191-5p and the PTEN 3' UTR. (**B**) Luciferase reporter activity of WT- or MUT-PTEN in U87 cells co-transfected with miRNA-191-5p mimics or miR-Control mimics. (**C**) Representative Western blot images showing the expression levels of PTEN in different treatment groups: miRNA-191-5p mimics or miR-control mimics, and miRNA-191-5p inhibitor or miR-control inhibitor. Densitometric analysis of band intensities was performed using ImageJ software. Protein levels were normalized to GAPDH and expressed as fold change relative to the control group. (**D**) Relative mRNA levels of PTEN in glioma cells transfected with miRNA-191-5p mimics or miR-control mimics, and miRNA-191-5p inhibitor or miR-control inhibitor. (**E**) Pearson correlation analysis between miR-191-5p and PTEN levels measured by qPCR in 40 primary glioma cases (r = 0.759, P < 0.0001). (**F**) Immunohistochemical (IHC) staining of PTEN in GSC-bearing xenografts treated with miR-191-5p agomir/antagomir or NC. Upper panels: scale bar = 100 μm; lower panels: scale bar = 25 μm, n = 3. Data were expressed as the mean ± SEM(repetition = 3); NS not statistically significant; *P < 0.05; **P < 0.01;***P < 0.001; ****P < 0.0001 according to two-tailed Student t tests used for two-group comparisons.
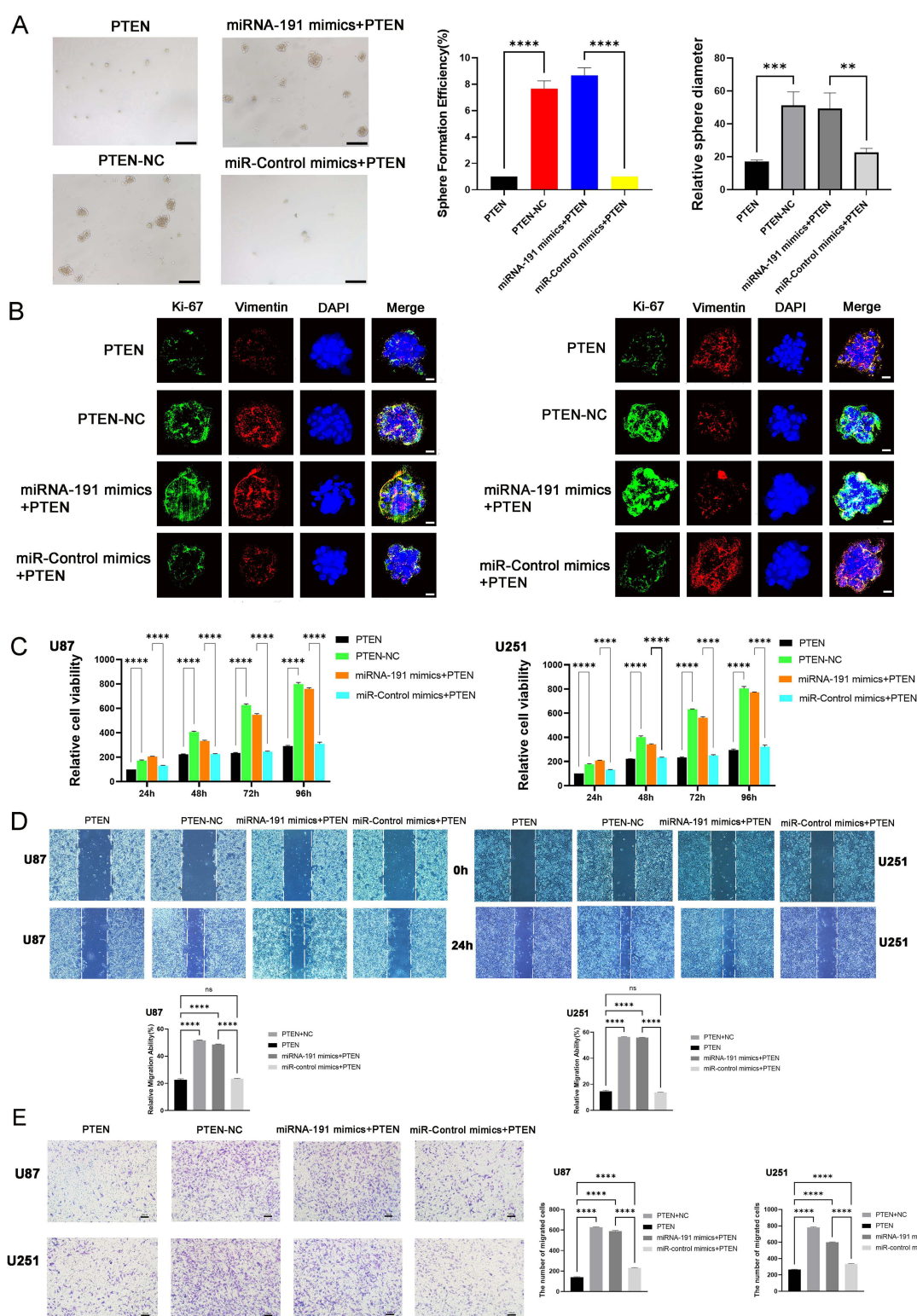
Figure 7 Restoration of PTEN Attenuates miRNA-191-5p Induced Tumorigenicity and PMT in Glioma Cells. (**A**) Representative bright field microscopy images display sphere formation in GSCs treated with miR-191 mimics and PTEN plasmids. Scale bar = 200 μm. Left: statistics of sphere formation; right: quantification of sphere diameter. (**B**) Immunofluorescence (IF) imaging shows Ki-67 and Vimentin/Sox2 expression in GSC tumorspheres co-transfected with miR-191-5p mimics and PTEN plasmids. (**C**) Cell proliferation in glioma cells was assessed by CCK-8 assays after co-transfection with PTEN plasmids and miRNA-191-5p mimics or miR-control mimics. (**D**) Migration of glioma cells measured by Wound healing assays following co-transfection with PTEN plasmids and miRNA-191-5p mimics or miR-control mimics. (**E**) Invasion of glioma cells was evaluated by Transwell assays after co-transfection with PTEN plasmids and miRNA-191-5p mimics or miR-control mimics. Data were expressed as the mean ± SEM (repetition = 3); NS not statistically. Significant; **P < 0.01; ***P < 0.001; ****P < 0.0001 according to two-tailed Student t tests or one-way ANOVA followed by Dunnett tests for multiple comparisons.
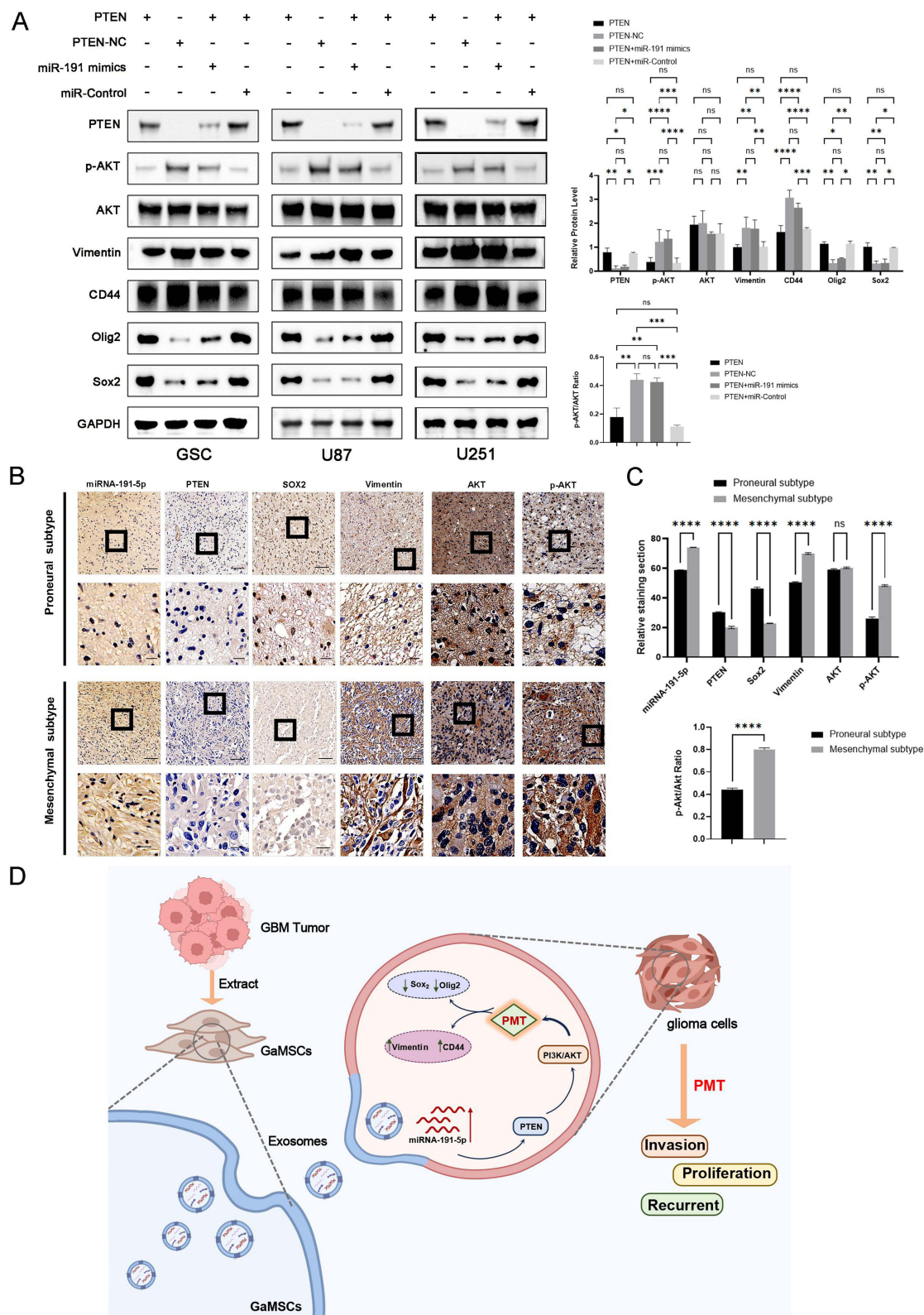
Figure 8 miRNA-191-5p Promotes PMT by Targeting PTEN Through the PI3K/Akt Signaling Pathway. (**A**) Western blot analysis of PTEN, Akt protein levels, phosphorylation, and PMT-related markers (Olig2, Sox2, Vimentin, and CD44) in glioma cells transfected with PTEN plasmids, miR-191-5p mimics, or miR-control mimics.Densitometric analysis of band intensities was performed using ImageJ software. Protein levels were normalized to GAPDH and expressed as fold change relative to the control group. (**B** and **C**) Relative expression levels of miRNA-191-5p, PTEN, Sox2, Vimentin, Akt, phosphorylated-Akt and p-Akt/Akt ratio in proneural and mesenchymal GBM as revealed by IHC and DAB-ISH staining. Representative images are shown (upper panels: scale bar = 100 µm; lower panels: scale bar = 25 µm). (**D**) Exosomes secreted from GaMSCs carrying miR-191-5p promotes glioma PMT by targeting PTEN and activating the PI3K/Akt signaling pathway, evidenced by elevation of Vimentin and CD44, and abaissement of Olig2 and Sox2. Data are presented as mean ± SEM; NS denotes not statistically significant; *P < 0.05; **P < 0.01; ***P < 0.001; ****P < 0.0001, as determined by two-tailed Student's t-tests or one-way ANOVA followed by Dunnett's tests for multiple comparisons.

191-5p and Vimentin in the mesenchymal subtype of GBM, whereas decreased levels of PTEN and Sox2 were observed compared to the proneural subtype. Additionally, the p-Akt/Akt ratio was also higher in the mesenchymal subtype than in the proneural subtype (Figure 8B and C). All of the aforementioned researches indicated that GaMSCs-Exos carrying miRNA-191-5p promote glioma PMT progression by targeting PTEN and activating the PI3K/Akt signaling pathway, leading to increased levels of Vimentin and CD44 and decreased levels of Olig2 and Sox2 (Figure 8D).

Discussion

In our study, we initially observed that the conditions provided by GaMSCs-CM enhance the proliferation and invasion of glioblastoma cells. Delving deeper into cellular communication mechanisms, we investigated the role of exosomes. Our findings reveal that exosomes derived from GaMSCs not only stimulate glioma cell proliferation but also facilitate PMT in glioblastoma cells. These outcomes underscore the intricate interactions between exosomes from GaMSCs and the tumor microenvironment, particularly highlighting their role in promoting PMT via the transfer of miRNA-191-5p, which targets PTEN through the PI3K/Akt signaling pathway (Figure 8D).

Since 2014, our team has illuminated the role of GaMSCs within the tumor niche in contributing to glioma development and progression, and their presence in high-grade gliomas is associated with decreased patient survival.[28] GaMSCs enhance proliferation and maintain the stemness of GSCs via the IL-6/gp130/STAT3 signaling pathway.[12] Moreover, GaMSCs possess potent immunosuppressive properties, inducing PD-L1 upregulation.[22] This study extends our understanding of GaMSCs' impact on PMT in glioblastoma through exosomal communication.

Based on the plasticity of MSCs, which can be influenced by manual manipulation or TME, leading to the release of extracellular vesicles containing various miRNAs and influence the progression of GBM. For instance, Zhan et al demonstrated that MSC-derived exosomes equipped with miR-1208 inhibit the malignant progression of glioma.[29] Similarly, Wang et al reported that MSCs shuttle miR-503 via extracellular vesicles, thereby enhancing glioma's immune escape.[30] GaMSCs-Exos, serving as crucial vehicles of "cross-talk" in the TME and contributing to the progression of gliomas, are underscored by a recent literature. It confirmed that miRNA-1578 exosomes originating from GaMSCs heighten the tumorigenicity of glioma stem-like cells.[18] Our study further observed that GaMSC-Exos enhance both the tumorigenicity and the PMT in glioma cells, suggesting a critical role of GaMSCs in facilitating PMT.

miRNA-191-5p is overexpressed in several solid tumors, including intrahepatic cholangiocarcinoma, hepatocellular carcinoma, colorectal cancer, and breast cancer, acting as a tumor promoter by enhancing cell proliferation, invasion, and metastasis, and by inhibiting apoptosis.[31–34] A specific study identified a set of miRNAs associated with outcomes across different glioblastoma subtypes, highlighting miRNA-191 as a prognostic marker for the mesenchymal subtype.[35] In our investigation, utilizing the GEO/CGGA database, we confirmed elevated levels of miRNA-191-5p in glioblastoma tissues compared to normal brain tissues, with increased expression correlating with higher glioblastoma grades (Figure 4). Our study also verified the high expression of miRNA-191-5p in GaMSC-Exos. The overexpression of GaMSC-Exos and miRNA-191-5p significantly enhances the tumorigenicity of glioma cells both in vivo and in vitro. This overexpression also upregulates the protein levels of mesenchymal markers (CD44 and Vimentin) while suppressing the expression of proneural markers (Olig2 and Sox2) in GBM cells. These findings further confirm that GaMSCs promote PMT in glioma cells by transporting miRNA-191-5p via GaMSC-Exos.

The target genes of miR-191 may exhibit tissue-specificity, varying according to the type of cancer. It targets TET1 in intrahepatic cholangiocarcinoma, SATB1 in breast cancer, beta-catenin in lung cancer, and CDK6 in thyroid follicular tumors.[31,33,36,37] In our studies, the 3′-UTR of PTEN contains complementary sequences matching the seed sequence of miR-191-5p. Our dual-luciferase reporter assay indicates that miRNA-191-5p directly interacts with PTEN in glioma. PTEN is a tumor suppressor gene and plays a crucial negative regulator in modulating the PI3K/Akt signaling pathway by its ability to dephosphorylate PI3K.[38] Recent research has revealed that exosomal miR-26a influences the PTEN/PI3K/AKT pathways, thereby facilitating angiogenesis in glioma.[27] In lung cancer, miRNA-21 can suppresses PTEN expression and enhance the invasiveness of cancer cells.[39] Further investigations have underscored the significance of the PTEN/PI3K/Akt signaling pathway in various aspects of tumor biology, including proliferation and EMT. Moreover, inhibitors such as valproic acid and Tyroservatide, which target the PTEN/PI3K/AKT signaling axis, have demonstrated therapeutic efficacy in various malignancies.[40,41] Thus, these inhibitors may represent a viable therapeutic approach in

glioma treatment. Recent advancements in artificial intelligence (AI) have introduced new methodologies for analyzing exosomal miRNA networks and their roles in cancer signaling pathways. AI-based models can simulate interactions within the PTEN/PI3K/Akt axis and predict therapeutic outcomes, potentially expediting the discovery of novel targets and enhancing personalized treatment strategies.[42–45]

PMT is now widely recognized as a key process in the advancement of gliomas, involving complex molecular and cellular changes, including alterations in gene expression, signaling pathways, and cell morphology.[4,46,47] Guo et al demonstrated that activated neurons release exosomes containing miR-184-3p, which promoted the growth and radio-resistance of glioblastoma by inducing PMT.[48] Zhang et al identified specific microRNAs (miR-27a-3p, miR-22-3p, and miR-221-3p) delivered by macrophage-derived extracellular vesicles that enhance the process of PMT in GSCs.[49] Our research provides additional evidence that GaMSC-Exos carrying miRNA-191-5p act as mediators promoting this transition. Elucidating the molecular mechanisms by which exosomal miRNA-191 induces PMT in GBM opens avenues for therapeutic exploration. Targeting this specific exosomal cargo or modulating the miRNA-191/PTEN/PI3K/AKT signaling pathway may offer innovative strategies to inhibit glioma progression.

However, our study has limitations. We specifically focused on the effect of GaMSC-Exos-derived miRNAs on PMT in GBM, whereas the TME consists of various stromal cells, extracellular vesicles, and cytokines that collectively influence tumor behavior. Future research should explore the broader regulatory roles of the TME in modulating PMT and glioma progression. Understanding the potential interactions between the TME and PMT in GBM could provide valuable insights into the mechanisms of glioblastoma progression and identify potential therapeutic targets.

Conclusions

In conclusion, our study highlights the pivotal role of GaMSCs-derived exosomes (GaMSCs-Exos) in PMT in GBM through the delivery of miR-191-5p, which targets PTEN. The activation of the PTEN/PI3K/AKT signaling axis supports the aggressive phenotypes associated with PMT and contributes to the progression of GBM. These findings not only enhance our understanding of the molecular mechanisms underlying PMT but also suggest potential therapeutic approaches aimed at disrupting key signaling pathways that drive glioma malignancy.

Abbreviations

GBM, Glioblastoma; GSCs, Glioma stem cells; PMT, The proneural to mesenchymal transition; GaMSCs, Glioma-associated mesenchymal stromal/stem cells; GaMSCs-Exos, Exosomes released from GaMSCs; GaMSCs-CM, GaMSCs Conditioned medium; MSCs, Mesenchymal stem cells; IF, Immunofluorescence; IHC, Immunohistochemistry; GSCs, Glioma stem cells; ISH, DAB-In situ hybridization; TEM, The transmission electron microscopy; NTA, The nanoparticle tracking analysis; NanoFCM, Flow Nanoanalyzer; EMT, Epithelial-mesenchymal transition.

Data Sharing Statement

Publicly available datasets were analyzed in this study. These data can be found at GEO (https://www.ncbi.nlm.nih.gov/geo/) and CGGA (http://www.cgga.org.cn/). The microarray datasets generated and analyzed during the current study are not publicly available because of confidentiality requirements for subsequent experiments (exploring other roles of GaMSCs-Exos in the tumor microenvironment), but are available from the corresponding authors (Peng Fu and Wei Xiang) upon reasonable request.

Ethics Approval and Consent to Participate

This research received ethical approval from the Ethical Committee of Huazhong University of Science and Technology [2019]IEC(S561) and adhered to the Helsinki Declaration of the World Medical Association. Written informed consent was obtained from each patient. The animal study complied with ethical regulations and was approved by the Experimental Animal Ethics Committee of Huazhong University of Science and Technology (IACUC Number:3854). All experiments complied with the Chinese Law on Laboratory Animal Welfare (Guideline for Ethical Review of Animal Welfare, Standard number: GB/T 35892–2018).

Author Contributions

All authors made a significant contribution to the work reported, whether that is in the conception, study design, execution, acquisition of data, analysis and interpretation, or in all these areas; took part in drafting, revising or critically reviewing the article; gave final approval of the version to be published; have agreed on the journal to which the article has been submitted; and agree to be accountable for all aspects of the work.

Funding

Disclosure

The authors declare no competing interests in this work.

References

1. Bao Z, Zhang N, Niu W, et al. Exosomal miR-155-5p derived from glioma stem-like cells promotes mesenchymal transition via targeting ACOT12. *Cell Death Dis*. 2022;13(8):725. doi:10.1038/s41419-022-05097-w
2. Zhou Y, Wu W, Bi H, Yang D, Zhang C. Glioblastoma precision therapy: from the bench to the clinic. *Cancer Lett*. 2020;475:79–91. doi:10.1016/j.canlet.2020.01.027
3. Phillips HS, Kharbanda S, Chen R, et al. Molecular subclasses of high-grade glioma predict prognosis, delineate a pattern of disease progression, and resemble stages in neurogenesis. *Cancer Cell*. 2006;9(3):157–173. doi:10.1016/j.ccr.2006.02.019
4. Lin Z, Zhang Z, Zheng H, et al. Molecular mechanism by which CDCP1 promotes proneural-mesenchymal transformation in primary glioblastoma. *Cancer Cell Int*. 2022;22(1):151. doi:10.1186/s12935-021-02373-1
5. Mancini A, Colapietro A, Cristiano L, et al. Anticancer effects of ABTL0812, a clinical stage drug inducer of autophagy-mediated cancer cell death, in glioblastoma models. *Front Oncol*. 2022;12:943064. doi:10.3389/fonc.2022.943064
6. Li H, Yuan Y, Chen H, Dai H, Li J. Indoleamine 2,3-dioxygenase mediates the therapeutic effects of adipose-derived stromal/stem cells in experimental periodontitis by modulating macrophages through the kynurenine-AhR-NRF2 pathway. *Mol Metab*. 2022;66:101617. doi:10.1016/j.molmet.2022.101617
7. Lu Y, Song S, Jiang X, et al. miR675 accelerates malignant transformation of mesenchymal stem cells by blocking DNA mismatch repair. *Mol Ther-Nucl Acids*. 2019;14:171–183. doi:10.1016/j.omtn.2018.11.010
8. Xue BZ, Xiang W, Zhang Q, et al. CD90(low) glioma-associated mesenchymal stromal/stem cells promote temozolomide resistance by activating FOXS1-mediated epithelial-mesenchymal transition in glioma cells. *Stem Cell Res Ther*. 2021;12(1):394. doi:10.1186/s13287-021-02458-8
9. Zhang Q, Xiang W, Yi DY, et al. Current status and potential challenges of mesenchymal stem cell-based therapy for malignant gliomas. *Stem Cell Res Ther*. 2018;9(1):228. doi:10.1186/s13287-018-0977-z
10. Zhang Q, Xiang W, Xue B-Z, Yi D-Y, Zhao H-Y, Fu P. Growth factors contribute to the mediation of angiogenic capacity of glioma-associated mesenchymal stem cells. *Oncol Lett*. 2021;21(3):215. doi:10.3892/ol.2021.12476
11. Yi D, Xiang W, Zhang Q, et al. Human glioblastoma-derived mesenchymal stem cell to pericytes transition and angiogenic capacity in glioblastoma microenvironment. *Cell Physiol Biochem*. 2018;46(1):279–290. doi:10.1159/000488429
12. Hossain A, Gumin J, Gao F, et al. Mesenchymal stem cells isolated from human gliomas increase proliferation and maintain stemness of glioma stem cells through the IL-6/gp130/STAT3 pathway. *Stem Cells*. 2015;33(8):2400–2415. doi:10.1002/stem.2053
13. Guo KT, Fu P, Juerchott K, et al. The expression of Wnt-inhibitor DKK1 (Dickkopf 1) is determined by intercellular crosstalk and hypoxia in human malignant gliomas. *J Cancer Res Clin*. 2014;140(8):1261–1270. doi:10.1007/s00432-014-1642-2
14. Zhang Q, Yi DY, Xue BZ, et al. CD90 determined two subpopulations of glioma-associated mesenchymal stem cells with different roles in tumour progression. *Cell Death Dis*. 2018;9(11):1101. doi:10.1038/s41419-018-1140-6
15. Hade MD, Suire CN, Suo Z. Mesenchymal stem cell-derived exosomes: applications in regenerative medicine. *Cells-Basel*. 2021;10(8). doi:10.3390/cells10081959
16. Khan FH, Reza MJ, Shao YF, et al. Role of exosomes in lung cancer: a comprehensive insight from immunomodulation to theragnostic applications. *Bba-Rev Cancer*. 2022;1877(5):188776. doi:10.1016/j.bbcan.2022.188776
17. Kahlert C, Kalluri R. Exosomes in tumor microenvironment influence cancer progression and metastasis. *J Mol Med*. 2013;91(4):431–437. doi:10.1007/s00109-013-1020-6
18. Figueroa J, Phillips LM, Shahar T, et al. Exosomes from glioma-associated mesenchymal stem cells increase the tumorigenicity of glioma stem-like cells via transfer of miR-1587. *Cancer Res*. 2017;77(21):5808–5819. doi:10.1158/0008-5472.CAN-16-2524
19. Zhou X, Zheng C, Shi Q, Li X, Shen Z, Yu R. Isolation, cultivation and identification of brain glioma stem cells by magnetic bead sorting. *Neural Regen Res*. 2012;7(13):985–992. doi:10.3969/j.issn.1673-5374.2012.13.004
20. Luo M, Liu YQ, Zhang H, et al. Overexpression of carnitine palmitoyltransferase 1A promotes mitochondrial fusion and differentiation of glioblastoma stem cells. *Lab Invest*. 2022;102(7):722–730. doi:10.1038/s41374-021-00724-0
21. Zhou Y, Meng X, He W, et al. USF1/CD90 signaling in maintaining glioblastoma stem cells and tumor-associated macrophages adhesion. *Neuro-Oncology*. 2022;24(9):1482–1493. doi:10.1093/neuonc/noac063
22. Zhang Q, Zhang J, Wang P, Zhu G, Jin G, Liu F. Glioma-associated mesenchymal stem cells-mediated PD-L1 expression is attenuated by Ad5-Ki67/IL-15 in GBM treatment. *Stem Cell Res Ther*. 2022;13(1):284. doi:10.1186/s13287-022-02968-z
23. Wang H, Feng X, Zhang Y, et al. PbUGT72AJ2-mediated glycosylation plays an important role in lignin formation and stone cell development in pears (Pyrus bretschneideri). *Int J Mol Sci*. 2022;23(14). doi:10.3390/ijms23147893

24. He S, Chu J, Wu LC, et al. MicroRNAs activate natural killer cells through toll-like receptor signaling. *Blood*. 2013;121(23):4663–4671. doi:10.1182/blood-2012-07-441360

25. Keller M, Blom M, Conze LL, Guo M, Hagerstrand D, Aspenstrom P. Altered cytoskeletal status in the transition from proneural to mesenchymal glioblastoma subtypes. *Sci Rep-Uk*. 2022;12(1):9838. doi:10.1038/s41598-022-14063-7

26. Lin X, Tang X, Zheng T, Qiu J, Hua K. Long non-coding RNA AOC4P suppresses epithelial ovarian cancer metastasis by regulating epithelial-mesenchymal transition. *J Ovarian Res*. 2020;13(1):45. doi:10.1186/s13048-020-00644-5

27. Wang ZF, Liao F, Wu H, Dai J. Glioma stem cells-derived exosomal miR-26a promotes angiogenesis of microvessel endothelial cells in glioma. *J Exp Clin Canc Res*. 2019;38(1):201. doi:10.1186/s13046-019-1181-4

28. Shahar T, Rozovski U, Hess KR, et al. Percentage of mesenchymal stem cells in high-grade glioma tumor samples correlates with patient survival. *Neuro-Oncology*. 2017;19(5):660–668. doi:10.1093/neuonc/now239

29. Zhan Y, Song Y, Qiao W, et al. Focused ultrasound combined with miR-1208-equipped exosomes inhibits malignant progression of glioma. *Br J Cancer*. 2023;129(7):1083–1094. doi:10.1038/s41416-023-02393-w

30. Wang XS, Yu XJ, Wei K, et al. Mesenchymal stem cells shuttling miR-503 via extracellular vesicles enhance glioma immune escape. *Oncoimmunology*. 2022;11(1):1965317. doi:10.1080/2162402X.2021.1965317

31. Li H, Zhou ZQ, Yang ZR, et al. MicroRNA-191 acts as a tumor promoter by modulating the TET1-p53 pathway in intrahepatic cholangiocarcinoma. *Hepatology*. 2017;66(1):136–151. doi:10.1002/hep.29116

32. Qin S, Zhu Y, Ai F, et al. MicroRNA-191 correlates with poor prognosis of colorectal carcinoma and plays multiple roles by targeting tissue inhibitor of metalloprotease 3. *Neoplasma*. 2014;61(1):27–34.

33. Nagpal N, Ahmad HM, Molparia B, Kulshreshtha R. MicroRNA-191, an estrogen-responsive microRNA, functions as an oncogenic regulator in human breast cancer. *Carcinogenesis*. 2013;34(8):1889–1899. doi:10.1093/carcin/bgt107

34. Shen J, Dicioccio R, Odunsi K, Lele SB, Zhao H. Novel genetic variants in miR-191 gene and familial ovarian cancer. *Bmc Cancer*. 2010;10:47. doi:10.1186/1471-2407-10-47

35. Li R, Gao K, Luo H, et al. Identification of intrinsic subtype-specific prognostic microRNAs in primary glioblastoma. *J Exp Clin Canc Res*. 2014;33(1):9. doi:10.1186/1756-9966-33-9

36. Xu W, Ji J, Xu Y, et al. MicroRNA-191, by promoting the EMT and increasing CSC-like properties, is involved in neoplastic and metastatic properties of transformed human bronchial epithelial cells. *Mol Carcinog*. 2015;54:E148–61. doi:10.1002/mc.22221

37. Colamaio M, Borbone E, Russo L, et al. miR-191 down-regulation plays a role in thyroid follicular tumors through CDK6 targeting. *J Clin Endocr Metab*. 2011;96(12):E1915–24. doi:10.1210/jc.2011-0408

38. Xu F, Liu G, Wang L, Wang X, Jin X, Bo W. miR-494 promotes progression of retinoblastoma via PTEN through PI3K/AKT signaling pathway. *Oncol Lett*. 2020;20(2):1952–1960. doi:10.3892/ol.2020.11749

39. Zhang JG, Wang JJ, Zhao F, Liu Q, Jiang K, Yang GH. MicroRNA-21 (miR-21) represses tumor suppressor PTEN and promotes growth and invasion in non-small cell lung cancer (NSCLC). *Clin Chim Acta*. 2010;411(11–12):846–852. doi:10.1016/j.cca.2010.02.074

40. Li C, Liu S, Gao J, et al. Epigenetic activation of PTEN by valproic acid inhibits PI3K/AKT signaling and Burkitt lymphoma cell growth. *Gene*. 2025;950:149369. doi:10.1016/j.gene.2025.149369

41. Qiu L, Gao Q, Liao Y, Li X, Li C. Targeted inhibition of the PTEN/PI3K/AKT pathway by YSV induces cell cycle arrest and apoptosis in oral squamous cell carcinoma. *J Transl Med*. 2025;23(1):145. doi:10.1186/s12967-025-06169-z

42. Habeeb M, Vengateswaran HT, You HW, Saddhono K, Aher KB, Bhavar GB. Nanomedicine facilitated cell signaling blockade: difficulties and strategies to overcome glioblastoma. *J Mater Chem B*. 2024;12(7):1677–1705. doi:10.1039/d3tb02485g

43. Khalighi S, Reddy K, Midya A, Pandav KB, Madabhushi A, Abedalthagafi M. Artificial intelligence in neuro-oncology: advances and challenges in brain tumor diagnosis, prognosis, and precision treatment. *Npj Precis Oncol*. 2024;8(1):80. doi:10.1038/s41698-024-00575-0

44. Awuah WA, Ben-Jaafar A, Roy S, et al. Predicting survival in malignant glioma using artificial intelligence. *Eur J Med Res*. 2025;30(1):61. doi:10.1186/s40001-025-02339-3

45. Habeeb M, You HW, Umapathi M, Ravikumar KK, Hariyadi Mishra S. Strategies of artificial intelligence tools in the domain of nanomedicine. *J Drug Deliv Sci Tec*. 2024;91. doi:10.1016/j.jddst.2023.105157

46. Chen Z, Wang H, Zhang Z, et al. Cell surface GRP78 regulates BACE2 via lysosome-dependent manner to maintain mesenchymal phenotype of glioma stem cells. *J Exp Clin Canc Res*. 2021;40(1):20. doi:10.1186/s13046-020-01807-4

47. Sa JK, Chang N, Lee HW, et al. Transcriptional regulatory networks of tumor-associated macrophages that drive malignancy in mesenchymal glioblastoma. *Genome Biol*. 2020;21(1):216. doi:10.1186/s13059-020-02140-x

48. Guo X, Qiu W, Wang C, et al. Neuronal activity promotes glioma progression by inducing proneural-to-mesenchymal transition in glioma stem cells. *Cancer Res*. 2024;84(3):372–387. doi:10.1158/0008-5472.CAN-23-0609

49. Zhang Z, Xu J, Chen Z, et al. Transfer of MicroRNA via macrophage-derived extracellular vesicles promotes proneural-to-mesenchymal transition in glioma stem cells. *Cancer Immunol Res*. 2020;8(7):966–981. doi:10.1158/2326-6066.CIR-19-0759